CHAPTER IV

RESULTS AND DISCUSSION

4.1 The physical properties of SBA-15

4.1.1 XRD patterns of pure silica SBA-15

XRD patterns of the as-synthesized and calcined SBA-15 are shown in Figure 4.1. Assignment of those peaks are known as (100), (110), and (200) reflections, respectively, which are the characteristic pattern of hexagonal mesoporous structures [10]. Peaks positions are located at quite low 2 theta values due to the lack of short-range order of its structure. After calcined in air at 550°C for 5 h, the XRD pattern shows that the hexagonal structure is still remained and peak intensity at (100) reflection increases which is resulted from the removal of triblock copolymer template from the pores of materials. Notice that the XRD pattern of the calcined sample is slightly shifted to the larger angle because the unit cell contracted after heated at high temperature (550°C) [38].

4.1.2 Sorption properties of SBA-15

The adsorption isotherm and pore size distribution of calcined SBA-15 are shown in Figure 4.2. It exhibits a type IV adsorption isotherm which is a characteristic pattern of mesoporous materials. Considering the pore size distribution of resulted sample in Figure 4.2(b), narrow pore size distribution was found in SBA-15 at the pore diameter of 8.06 nm. The multipoint Brunauer, Emmett and Teller (BET) method was used in measuring total surface area of SBA-15, which was found at 684 m^2/g.

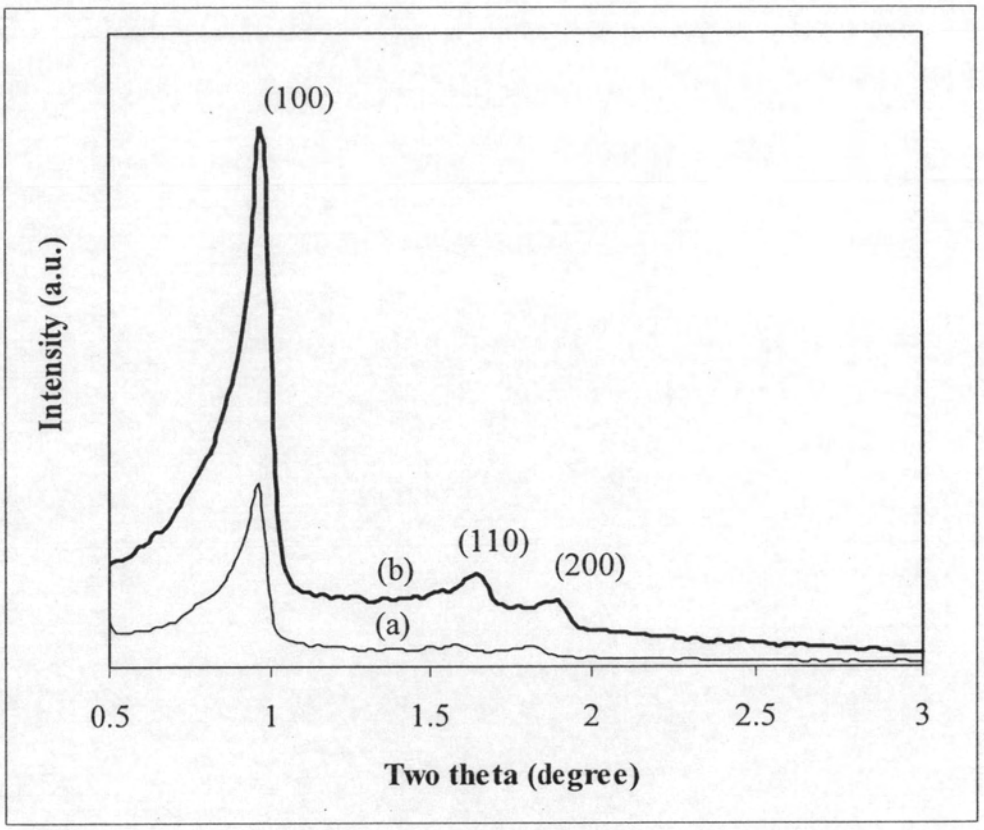

Figure 4.1 XRD patterns of (a) as-synthesized and (b) calcined pure silica SBA-15.

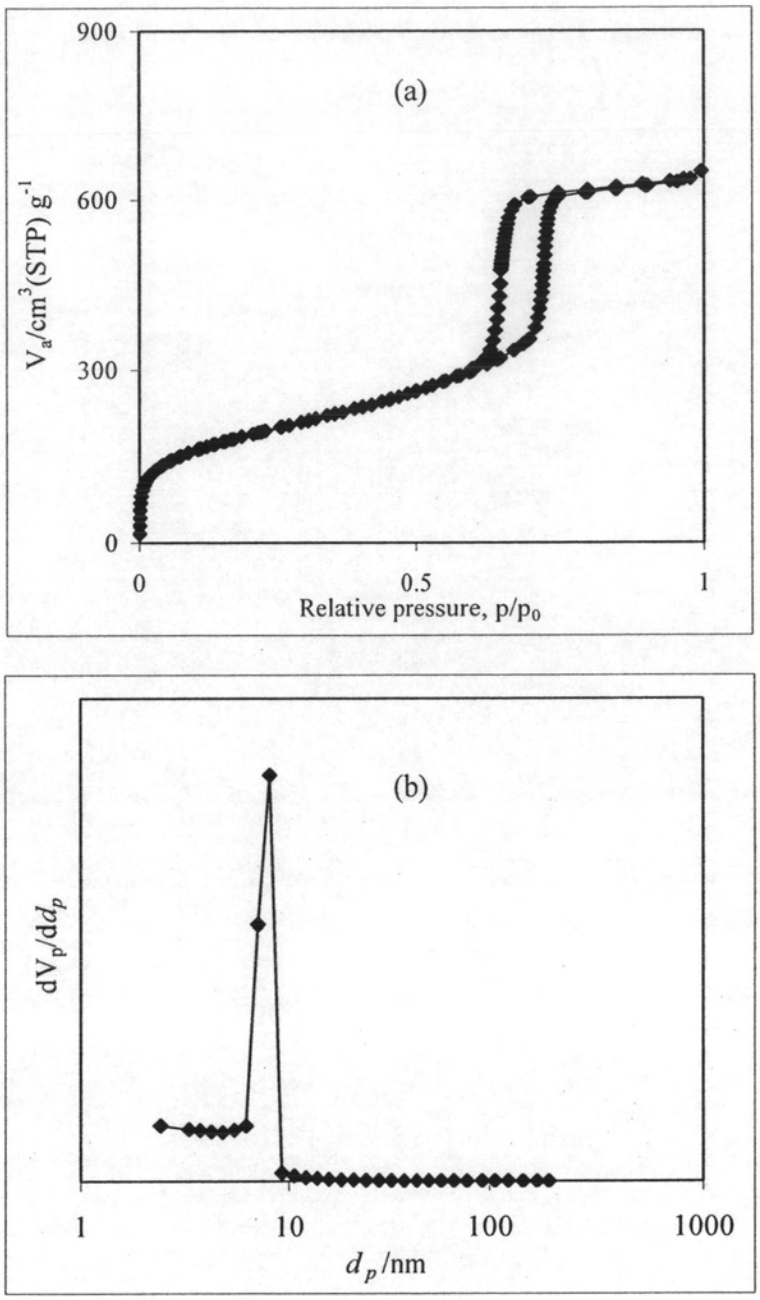

Figure 4.2 (a) Adsorption isotherm and (b) pore size distribution of SBA-15.

4.1.3 SEM images of SBA-15

SEM images of calcined pure silica SBA-15 at different magnifications are shown in Figure 4.3. The SEM images reveal that the calcined SBA-15 consists of small particle size of 80×116 nm, which are aggregated into rope like structure.

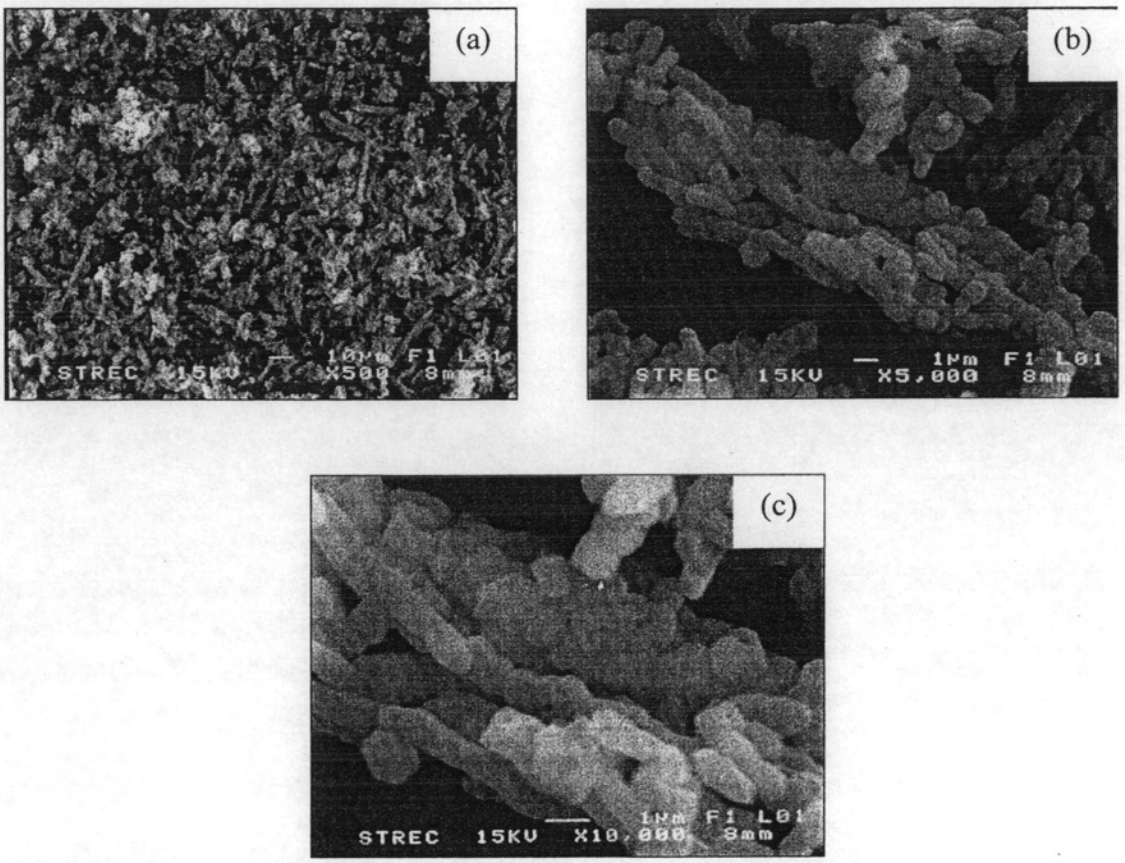

Figure 4.3 The SEM images of calcined pure silica SBA-15 at different magnifications (a) x500, (b) x5000, and (c) x10000.

4.2 The physico-chemical properties of Al-SBA-15

4.2.1 XRD patterns

In this report, two methods for synthesis of Al-SBA-15 with Si/Al ratios in reactant mixture of 10, 25, and 50 have been attempted: (i) Direct synthesis (D-Al-SBA-15); (ii) post synthesis (P-Al-SBA-15). The former method was performed according to Ooi and coworkers [37] and the latter was carried out by following Luan and coworkers [19]. XRD patterns of products prepared by direct synthesis (denoted as D-Al-SBA-15) are shown in Figure 4.4 and those prepared by post synthesis (P-Al-SBA-15) are shown in Figure 4.5. For all Al-SBA-15 products, similar three well-resolved peaks are observed. From both methods, the intensity of the (100) reflection increases when the Si/Al ratio in gel is increased. The result indicates that the lower the aluminum content, the higher order hexagonal structure is formed because the low aluminum content can be highly dispersed in the structure.

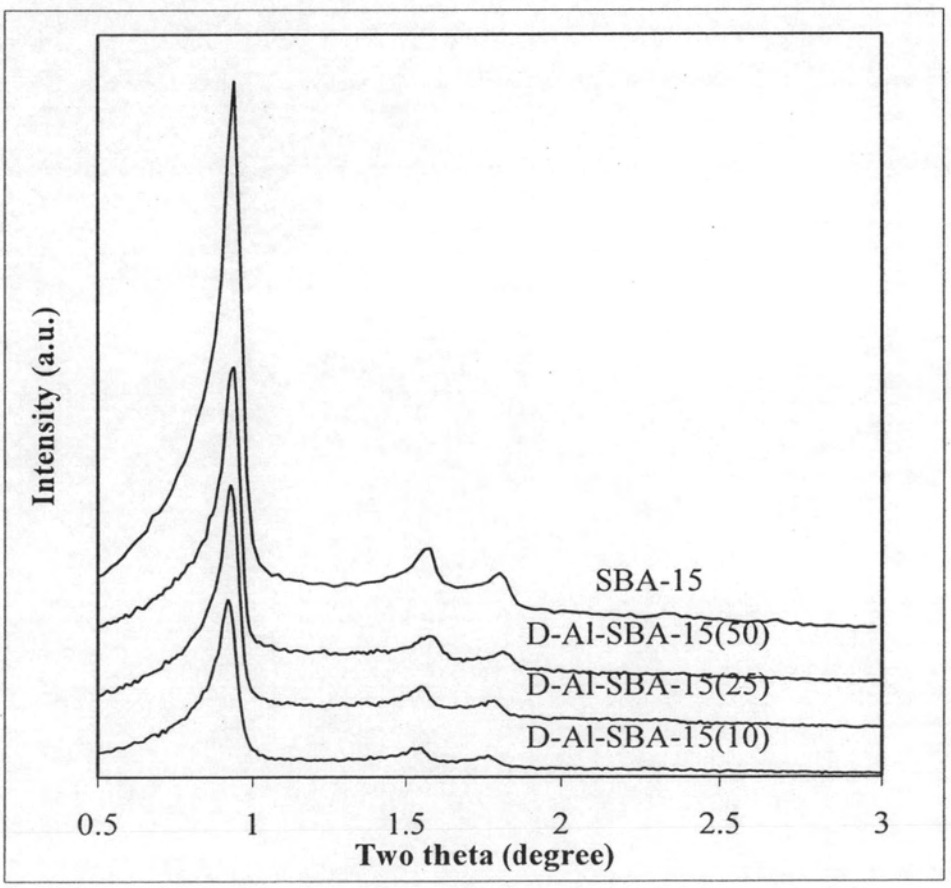

Figure 4.4 XRD patterns of Al-SBA-15 prepared by direct synthesis with various Si/Al ratios in reactant mixture.

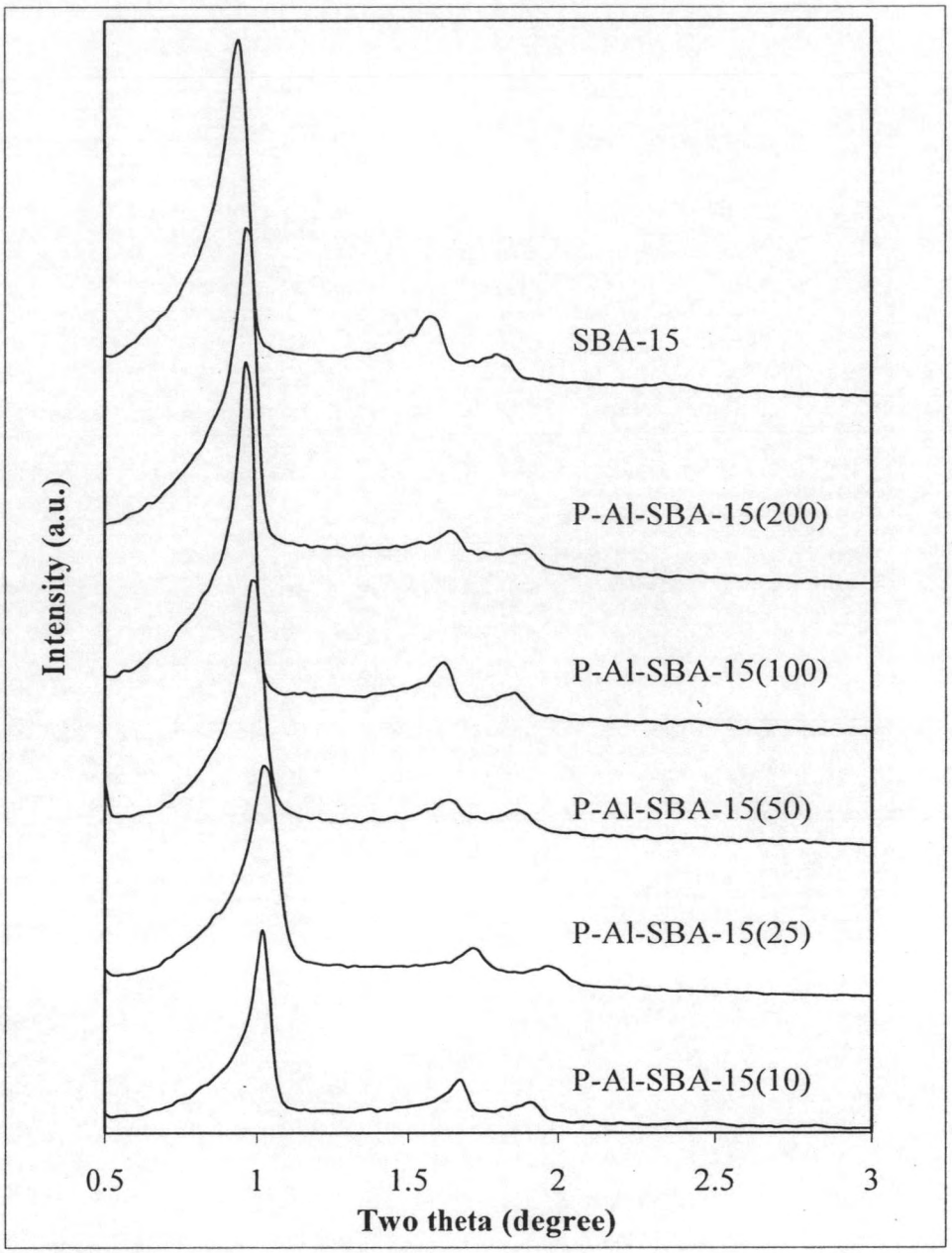

Figure 4.5 XRD patterns of Al-SBA-15 prepared by post synthesis with various Si/Al ratios in reactant mixture.

4.2.2 SEM images

SEM images of Al-SBA-15 samples prepared by direct and post synthesis methods are shown in Figure 4.6. Pure silica SBA-15 has a uniform particle size about 1 μm as presented in Figure 4.6 (a). Al-SBA-15(10) prepared by direct synthesis method (Figure 4.6 (b)) consists of featureless morphology while Al-SBA-15(10) (Figure 4.6 (c)) from post synthesis method shows uniform rod shape particles. The effect of aluminum addition caused the particles distribution different from that found for pure silica SBA-15 but the rod shape of individual particle remains the same.

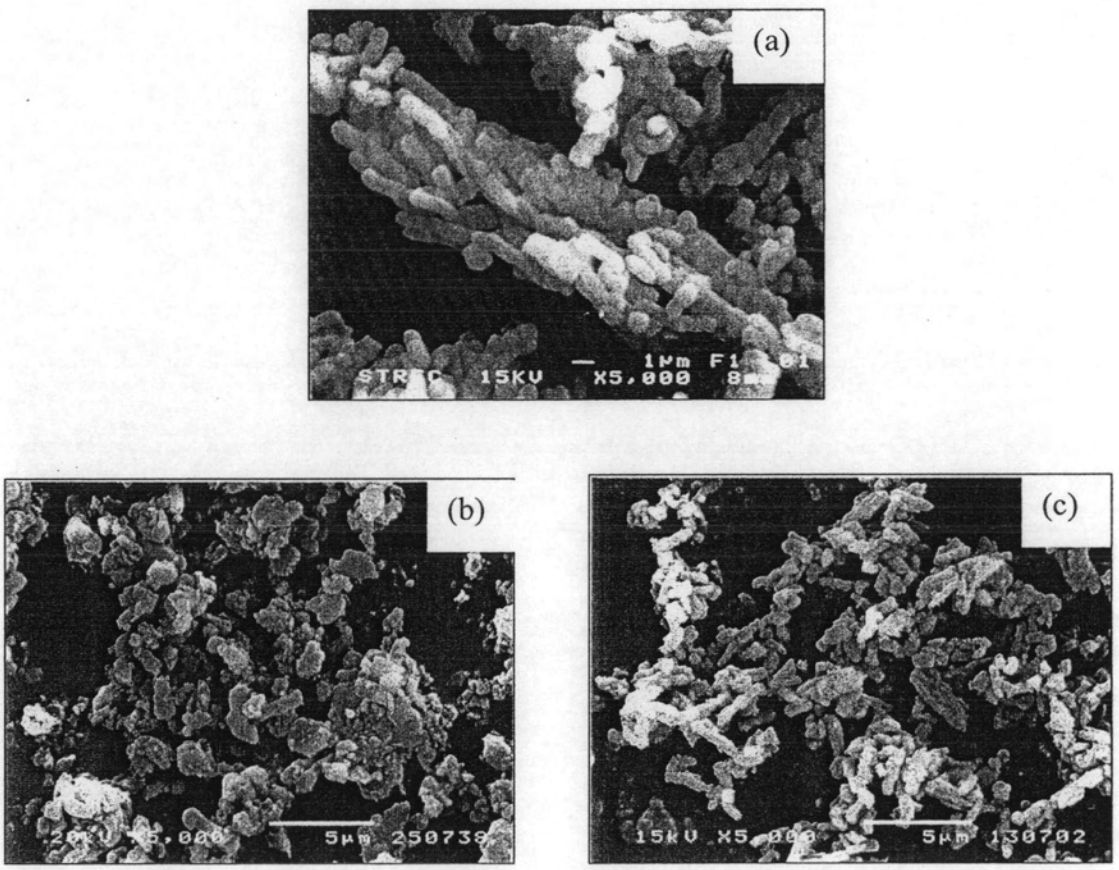

Figure 4.6 SEM images of (a) pure SBA-15, (b) D-Al-SBA-15 (Si/Al in gel = 10), and (c) P-Al-SBA-15 (Si/Al in reactant mixture = 10).

4.2.3 Si/Al ratios

The Si/Al ratios in gel and in product of the Al-SBA-15 prepared by both direct and post synthesis approaches are compared in Table 4.1. It is obvious that aluminum contents in catalyst prepared by direct synthesis are much greater than those prepared by post synthesis at the same Si/Al ratio in reactant mixture. The aluminum is difficult to be incorporated in the SBA-15 structure due to its high solubility in the acid media utilized in the direct synthesis method. This means that the direct synthesis method used in work is not appropriate for preparing aluminum-containing SBA-15.

However, the Si/Al molar ratios in the reactant mixture for Al-SBA-15 catalyst synthesized by post synthesis are less than those found in catalyst by half. The ratio reported in literature is varied depending laboratory procedure. In some cases the general method is the same, but there is perhaps some detail which may be different such as number of washing times after aluminum loading. The more times of washing, the less of remain aluminum content should be found. However, not all of the aluminum amount will be in tetrahedral framework position, if the loading is too high depending on the treatment.

From these results, it can be concluded that post synthesis is more proper to be used than direct synthesis. This is agreement with others [18-19]. However, data from only ICP-AES technique can not exhibit the position of aluminum atom, whether it located in framework or extra-framework, therefore data from ^{27}Al-NMR is needed for identification.

Table 4.1 Si/Al ratios in reactant mixture and in product of Al-SBA-15 samples.

Sample	Si/Al molar ratio	
	in reactant mixture	in catalyst
D-Al-SBA-15	10	384.20
D-Al-SBA-15	25	531.80
P-Al-SBA-15	10	10.75
P-Al-SBA-15	25	14.94
P-Al-SBA-15	50	30.36
P-Al-SBA-15	100	50.80
P-Al-SBA-15	200	107.04

4.2.4 ^{27}Al-MAS-NMR spectra of Al-SBA-15

Solid state ^{27}Al-MAS-NMR can provide the information of the aluminum atoms that they are located at the framework or non-framework site. The ^{27}Al-NMR spectra of calcined Al-SBA-15 samples prepared by post synthesis and treated with at least 2 M HNO_3 and 1-2 M NH_4Cl at various conditions are presented in Figures 4.7. The Al-SBA-15 samples used in this study exist in two intermediates that are wet sample (only filtered after post synthesis and dried sample (oven dried at 100°C overnight after post synthesis). It was on the hypothesis that both wet and dried samples still contain template but we can save time by using wet samples right after filtration without oven drying. To be assured that our hypothesis is correct, the treatment was performed on both wet and dried samples.

The ^{27}Al-MAS-NMR spectra of non ion-exchanged Al-SBA-15 (Na/H-Al-SBA-15) in Figure 4.7(a) exhibit only a signal at 55 ppm which is typically assigned to tetrahedral aluminum species. There is no peak at 0 ppm which belongs to octahedral aluminum species. However, it cannot tell whether the counter ions are totally H^+ or Na^+ as well. It is necessary to change sodium ions in catalyst to protons form in order to enhance the acid properties of Al-SBA-15 as described in Section 3.5. The ^{27}Al-MAS-NMR spectra of Al-SBA-15 samples treated with 2 M HNO_3 and 1-2 M NH_4Cl are presented in Figure 4.7 (b) to (e). It is obvious that both signals at 0 and 55 ppm are observed after acid and salt treatment. This can be explained that high concentration of treating reagents can cause leaching of aluminum in the framework site to the non framework site. In some zeolites (such as HY, HZSM-5 and zeolite beta) and mesoporous materials (such as Al-MCM-41 and Al-SBA-15) some framework aluminum species could also exist in the form of six-coordinate octahedral aluminum in the presence of water molecules. Although it can be converted to tetrahedral aluminum by adsorption of ammonia [17, 39-41], the details of the tetrahedral-to-octahedral conversion mechanism are still unclear. A partial of framework Al–O bonds is hydrolyzed to give framework-connected Al–OH species linked to two water molecules, generating octahedral aluminum species. It is interesting that, for conditions (c), (e), (f), and (g) a signal at *ca.* 30 ppm, maybe indicative of five-coordinate aluminum, can be observed. A similar behavior has been reported for Al-SBA-15 and AlMCM-41 materials [19, 42-43].

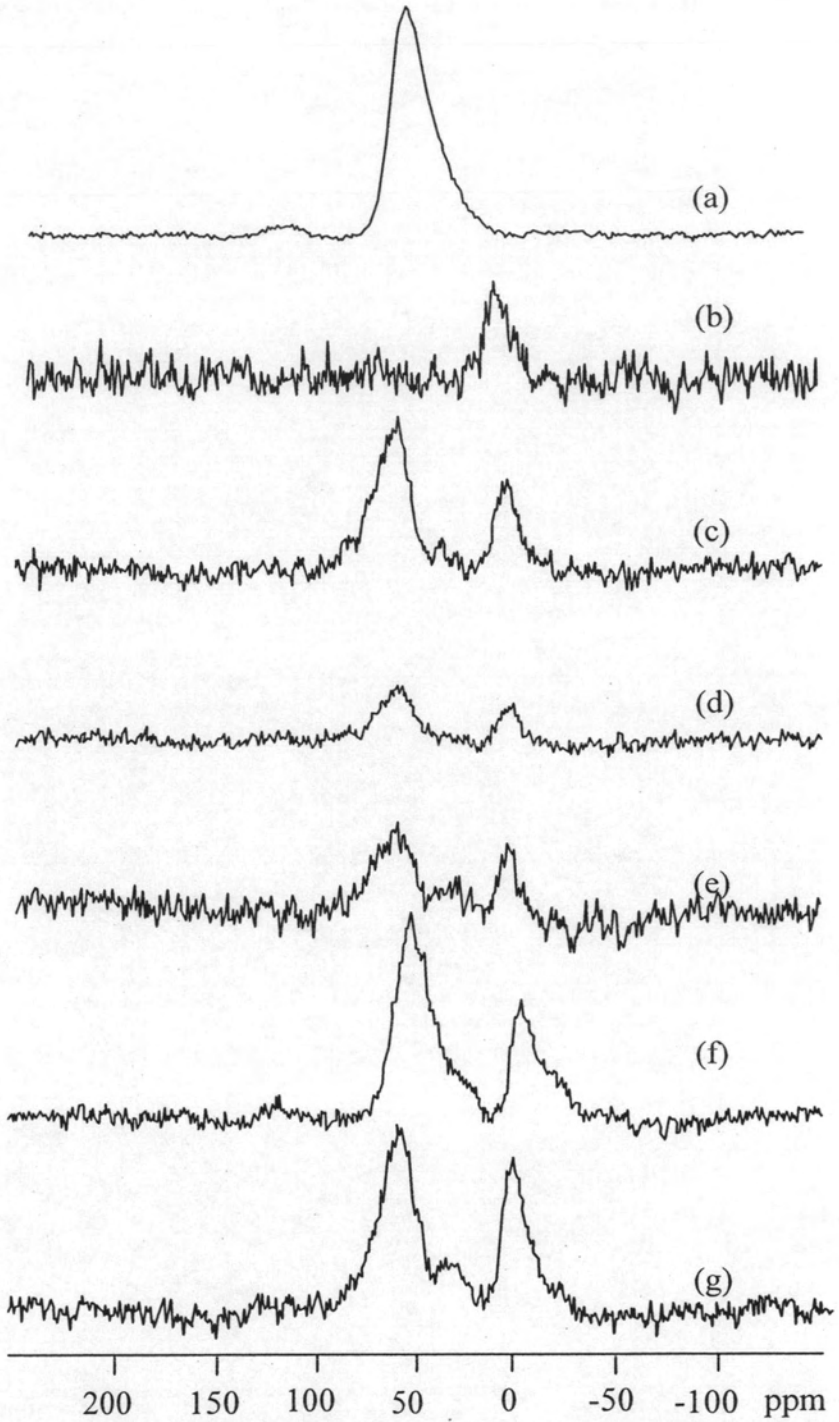

Figure 4.7 The ^{27}Al-MAS-NMR spectra of P-Al-SBA-15 (10) (a) non ion-exchanged, and P-Al-SBA-15 treated with (b) 2 M HNO_3, 24 h under reflux, (c) 2 M NH_4Cl, 24 h, under reflux (d) 1 M NH_4Cl, 24 h (wet sample), under reflux, (e) 1 M NH_4Cl, 12 h (wet sample) under reflux, (f) 1 M NH_4Cl, 12 h, under reflux and (g) 1 M NH_4Cl, 24 h, at room temperature.

The ^{27}Al-MAS-NMR spectra of P-Al-SBA-15 (10) treated with 0.01 M HNO_3 or 0.01 M NH_4Cl using whether wet or dried Al-SBA-15 samples are shown in Figure 4.8. All treated samples exhibit only one intense signal of the framework site at 50 ppm. Comparing Figure 4.8 (a) and (b), or (c) and (d), there is no difference in peak intensity between the cases treated with 0.01 M HNO_3 or 0.01 M NH_4Cl. Both 0.01 M HNO_3 and 0.01 M NH_4Cl can be used in the ion exchange of Al-SBA-15 but treatment of dried Al-SBA-15 sample is preferred. Obviously, the treated wet Al-SBA-15 samples show slightly lower intensity than those prepared with dried Al-SBA-15. Therefore, it is more proper to prepare H-Al-SBA-15 by ion exchange with 0.01 M NH_4Cl or HNO_3 using dried Al-SBA-15 materials.

When H-Al-SBA-15 with various Si/Al ratios were treated with 0.01 M HNO_3 or 0.01 M NH_4Cl and the ^{27}Al-MAS-NMR spectra of the treated samples are shown in Figure 4.9. It is obvious that the intensity of the signal at 55 ppm gradually increases with the increasing Al amount, indicating that the amount of Al atoms that are incorporated into the mesoporous wall of SBA-15 increasing as well. In contrast to other reports [42-43, 44] that ^{27}Al-MAS-NMR spectra of post synthesized Al-SBA-15 samples exhibited octahedral aluminum, no existence of octahedral aluminum in our result. All combined data suggest that aluminum atoms have been successfully incorporated into SBA-15 structure at purely tetrahedral framework position by following this post-synthesis alumination, drying, and subsequently ion exchange with 0.01 M HNO_3 or 0.01 M NH_4Cl..

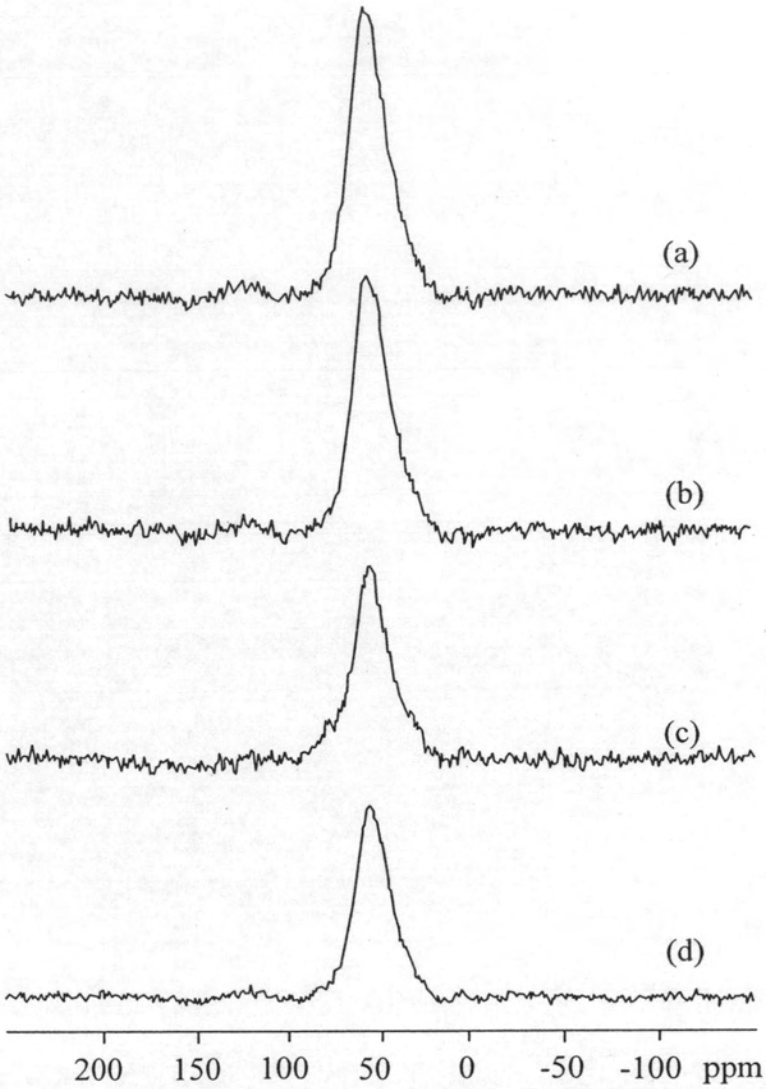

Figure 4.8 The ^{27}Al-MAS-NMR spectra of P-Al-SBA-15 (10) treated under reflux with (a) 0.01 M NH_4Cl, 24 h (dried sample), (b) 0.01 M HNO_3, 24 h (dried sample), (c) 0.01 M NH_4Cl, 24 h (wet sample), and (d) 0.01 M HNO_3, 24 h (wet sample).

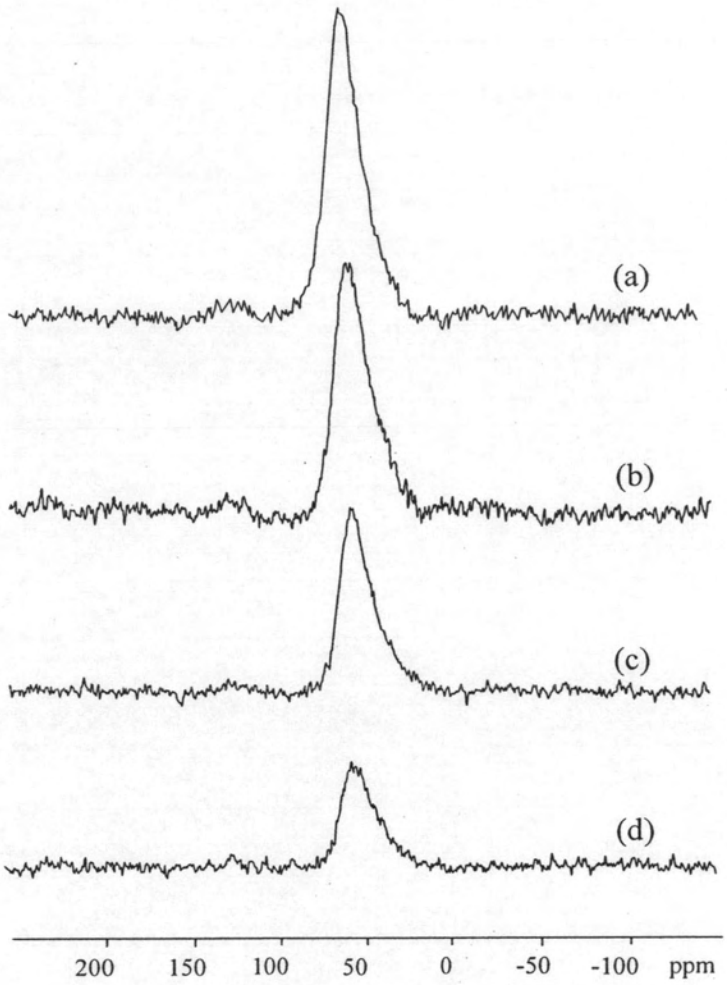

Figure 4.9 The ^{27}Al-MAS-NMR spectra of H-Al-SBA-15 materials ion exchanged with 0.01 M NH_4Cl with various Si/Al ratios: (a) H-Al-SBA-15(10), (b) H-Al-SBA-15(25), (c) H-Al-SBA-15(50) and (d) H-Al-SBA-15(100).

4.2.5 Sorption properties of Al-SBA-15

Nitrogen adsorption-desorption isotherms of the post synthesized Al-SBA-15 are shown in Figure 4.10. All samples exhibit hysteresis loop of type IV adsorption isotherms, typical for a mesoporous material. The BET specific surface areas are listed in Table 4.2. Incorporation of aluminum into the wall results in a decrease of the BET specific surface area. The more aluminum content, the less the BET specific surface area is. This result is in agreement with those in literature [16, 17, 37].

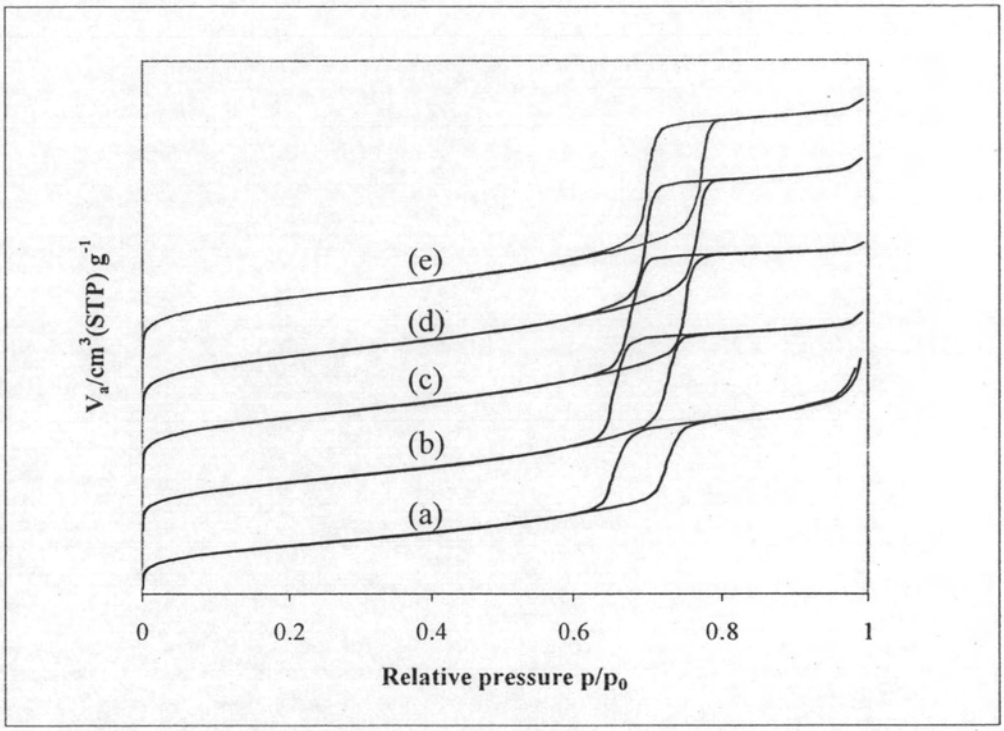

Figure 4.10 N_2 adsorption-desorption isotherm of (a) H-Al-SBA-15(10), (b) H-Al-SBA-15(15), (c) H-Al-SBA-15(30), (d) H-Al-SBA-15(50) and (e) H-Al-SBA-15(100) prepared by post synthesis.

Table 4.2 BET specific surface area of H-Al-SBA-15 prepared by post synthesis and ion exchange with 0.01M NH_4Cl compared with pure silica SBA-15

Sample	$a_{s, BET}$ (m^2/g)
SBA-15	684
H-Al-SBA-15(100)	613
H-Al-SBA-15(50)	603
H-Al-SBA-15(30)	571
H-Al-SBA-15(15)	505
H-Al-SBA-15(10)	440

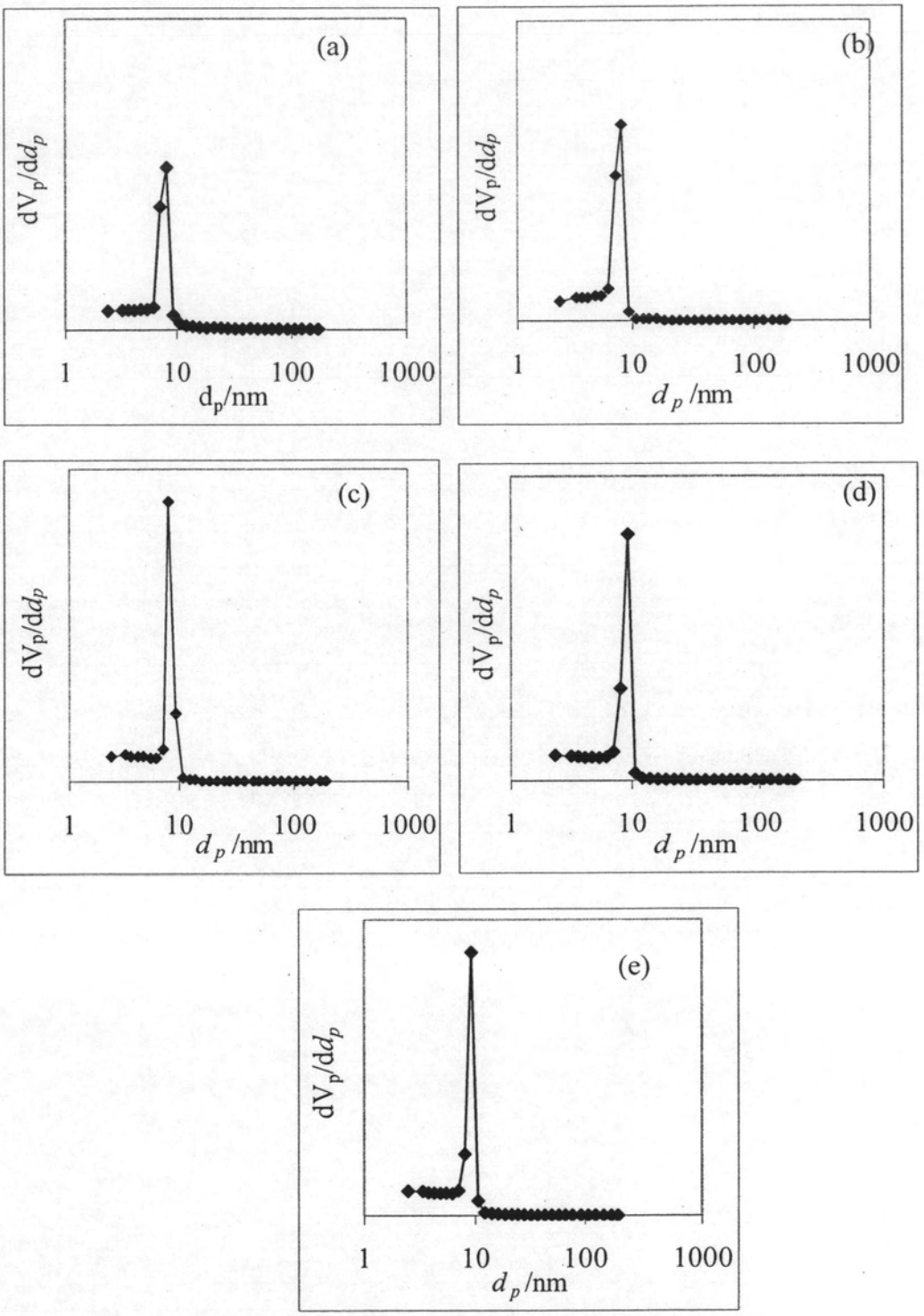

Figure 4.11 Pore size distribution of (a) H-Al-SBA-15(10), (b) H-Al-SBA-15(15), (c) H-Al-SBA-15(30), (d) H-Al-SBA-15(50) and (e) H-Al-SBA-15(100) prepared by post synthesis.

Pore size distributions of Al-SBA-15 are shown in Figure 4.11. All samples exhibit a narrow distribution with the pore size of 8.06 nm. By comparing to the pore size distribution of pure silica SBA-15 in Figure 4.2(b), the pore size of all H-Al-SBA-15 samples still remained unchanged, indicating the extreme stability of H-Al-SBA-15.

4.2.6 Acidity of H-Al-SBA-15

Ammonia TPD profiles of H-Al-SBA-15 with different Si/Al ratios are shown in Figure 4.12. The number of acid sites is related to a total amount of ammonia desorbed that is determined by the peak area. Acid strength of a sample is related to the temperature of desorbed ammonia. Each H-Al-SBA-15 sample prepared by the post synthesis method with various Si/Al ratios exhibit only one desorption peak with a maximum lower than 200°C, which is relatively lower than strong solid acid like zeolites. The acidity, both in term of acid strength and number of acid sites, of H-Al-SBA-15 increases with increasing aluminum content, *i. e.* the lower Si/Al molar ratio in the samples.

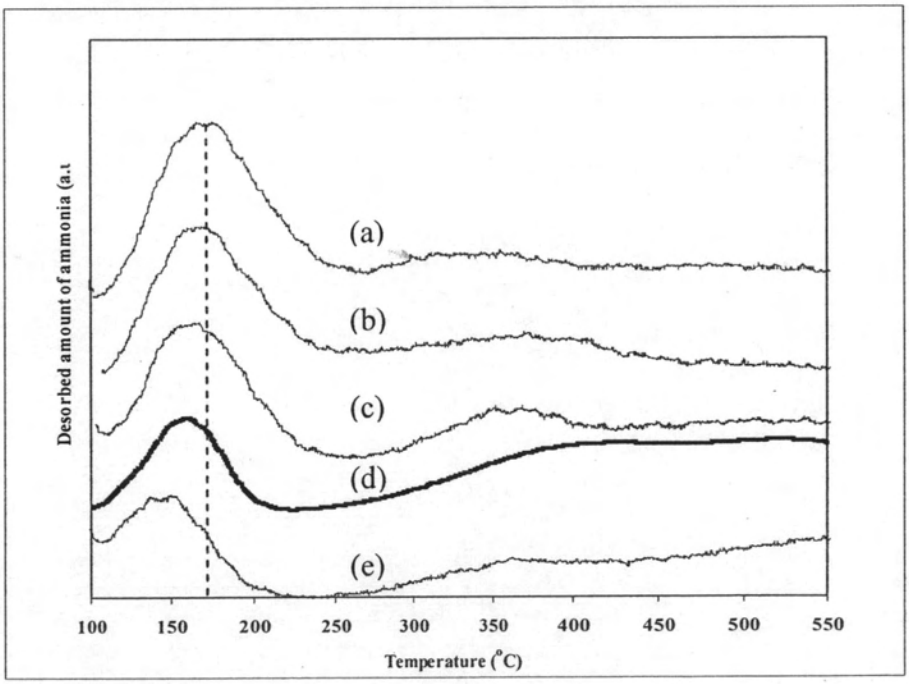

Figure 4.12 Ammonia TPD profiles of (a) H-Al-SBA-15(10), (b) H-Al-SBA-15(25), (c) H-Al-SBA-15(50), (d) H-Al-SBA-15(100), and (e) H-Al-SBA-15(200) prepared via post synthesis method, followed by ion exchange with 0.01 M NH_4Cl for 24 h.

4.3 Activity of SBA-15 and Al-SBA-15 in cracking of polypropylene

4.3.1 Effect of sodium ion in catalyst

The cracking of polypropylene over various catalysts: SBA-15, Na/H-Al-SBA-15(10), H-Al-SBA-15(10)-acid, and H-Al-SBA-15(10)-salt were performed at 380°C for 30 min, compared to thermal cracking without catalyst and the results are shown in Table 4.3. The catalysts are denoted as Na/H-Al-SBA-15(10) for non ion exchanged catalyst, H-Al-SBA-15(10)-acid for catalyst treated with 0.01 M HNO_3 for 24 h and H-Al-SBA-15(10)-salt for catalyst treated with 0.01 M NH_4Cl for 24 h.

Table 4.3 Conversion and product yield from thermal cracking of PP over SBA-15 and various Al-SBA-15(10) catalysts with different treatment compared to thermal cracking at 380°C (Condition: 10%wt catalyst of PP, N_2 flow of 20 cm^3/min and reaction time of 30 min)

	Thermal cracking	SBA-15	Na/H-Al-SBA-15(10)	H-Al-SBA-15-(10)-salt	H-Al-SBA-15(10)-acid
Conversion[a] (%)	29.40	13.00	92.60	97.00	97.20
Yield[b] (%)					
gas fraction	18.40	13.00	30.20	24.00	22.60
liquid fraction	11.00	0	62.40	73.00	74.60
residue	70.60	87.00	7.40	3.00	2.80
- wax	*70.60*	*87.00*	*6.63*	*2.15*	*2.18*
- solid coke	-	-	*0.77*	*0.85*	*0.62*

[a] *Deviation within 0.45%*
[b] *Deviation within 0.71%*

All Al-SBA-15(10) catalysts exhibit a high performance with the conversion of PP over 90% in all reactions with small amounts of residue. Considering product yield, catalytic cracking of PP over Al-SBA-15(10) catalysts produced higher liquid fraction than gas fraction. The yields of liquid fraction are in the range of 62-74% while that of gas fraction is about 22-30%. This can be explained by the milder acidity and larger pore size (80.6 Å) of these catalysts as compared to

zeolites, therefore, Al-SBA-15(10) shows the less degree of overcracking. It is found that all Al-SBA-15(10) catalysts show higher conversion than SBA-15 and thermal cracking. Thermal cracking gives low conversion about 29% with a large amount of residue but SBA-15 exhibits even lower conversion of only 13%. It is interesting that SBA-15 produces significantly lower PP conversion than thermal cracking. It has been reported by Hillhouse *et al.* [46] that SBA-15 is a good thermal insulator. Thus SBA-15 prevents the PP from readily undergoing thermal cracking. The result also indicates that pure silica SBA-15 cannot perform as a catalyst in cracking of PP. Incorporation of Al in the SBA-15 structure results in an increase in conversion of Al-SBA-15(10) from 13% to 92.60%. Treatment of Al-SBA-15(10) with either 0.01 M NH_4Cl or 0.01 M HNO_3 promotes the conversion by 4.4 or 4.6%, respectively. The presence of Na even in a small amount in the catalyst makes a decrease in activity of the acid catalyst in cracking of PP.

Thermal cracking of PP using the cracking apparatus set up in our laboratory promotes the higher conversion as compared to that of Aguadro *et al.* giving PP conversion only 8% at 400°C [13] and Miskolczi *et al.* giving PP conversion only 5.8% at 550°C [45]. It is noted that PP conversions from those two laboratories did not correspond to temperature. Thus, the comparison in conversion would rather be compared using the same reactor because the actual temperature of catalyst may be not the same as the temperature of the reactor. However, in general, it is difficult to measure the catalyst temperature, thus the reactor temperature was used instead and the thermocouple position is varied from laboratory to laboratory. Generally the catalyst temperature is lower than the reactor temperature. Our reactor was designed specifically to make the catalyst temperature very close to the reactor temperature, resulting in higher thermal cracking conversion compared to some other laboratories.

Thermal cracking provides 18.4% yield of gas fraction, 11% yield in yellow liquid fraction, and 70.60% in white waxy residue. Catalytic cracking of PP over Na/H-Al-SBA-15(10), H-Al-SBA-15(10)-salt, and H-Al-SBA-15(10)-acid catalysts gives 30.20, 24.0, and 22.60% yield in gas fraction, 62.40, 73.0, and 74.60% yield in pale yellow liquid fraction, and 7.40, 3.0, and 2.80% of residue, respectively. By thermal cracking the product in gas fraction is in higher yield than liquid fraction. In the presence of non-acid catalyst SBA-15, only small amount gas product and no liquid fraction were detected. An enormous amount of residue was left in the reactor

for both thermal cracking and cracking over SBA-15. In contrast to using Al-SBA-15(10) catalysts, the product in liquid fraction is in higher yield than gas fraction and residue yields are much less compared to thermal cracking and inactive SBA-15.

Residue, referred to all remaining in the reactor except catalyst, was identified as solid coke deposited on catalyst and wax. It is found at low conversion of 30% or less the residue is only white wax. At higher conversion residue in term of wax is decreased. The amounts of coke deposited on all Al-SBA-15(10) are quite low, less than 1%. This is a good sign of applying Al-SBA-15(10) as cracking catalyst.

The properties of liquid fraction corresponding to condition in Table 4.3 are shown in Table 4.4. Selectivity to light oil increases in the order of H-Al-SBA-15(10)-salt ≈ H-Al-SBA-15(10)-acid ≈ thermal cracking > Na/H-Al-SBA-15(10) while the heavy oil is in the opposite order, *i. e.* H-Al-SBA-15(10)-salt ≈ H-Al-SBA-15(10)-acid ≈ thermal cracking < Na/H-Al-SBA-15(10). Na/H-Al-SBA-15(10) has the highest density of liquid fraction compared to others and it accounts for the highest selectivity to heavy oil. The two fully acid Al-SBA-15(10) catalysts provide almost the same total volumes of liquid fraction and higher than the one with the presence of sodium. All three catalysts have much greater volume of liquid fraction compared to the case of thermal cracking.

Figure 4.13 shows the volume of liquid fraction accumulated in the graduated cylinder and the temperature in the reactor as a function of lapsed time for thermal cracking of PP over various Al-SBA-15(10) catalysts. This plots accounts for the kinetic rate of these reactions. No liquid product was obtained in the case of non acidic SBA-15. For thermal cracking no liquid was found in the graduate cylinder until 20 min past the point of reaching the required temperature of 380°C. It is obvious that the kinetic rate in liquid formation is very slow with the final accumulative volume of liquid only 1.30 cm^3. It indicates that the rate of reaction is drastically increased when Al-SBA-15(10) is ion exchanged with whether HNO_3 or NH_4Cl solutions. The rate of liquid formation for H-Al-SBA-15(10)-salt is the same as that for H-Al-SBA-15(10)-acid. Hence, it can be concluded that a small amount of sodium in catalyst still affects the rate of reaction; therefore, ion exchange is a necessary required to modify Al-SBA-15 catalyst.

Table 4.4 Properties of liquid fraction from cracking of PP over SBA-15 and various Al-SBA-15(10) catalysts with different treatment at 380°C (Condition: 10%wt catalyst of PP, N_2 flow of 20 cm^3/min and reaction time of 30 min)

Properties of liquid fraction	Thermal cracking	Na/H-Al-SBA-15(10)	H-Al- SBA-15(10)-salt	H-Al-SBA-15(10)-acid
Selectivity (%)				
- *light oil*	*36.84*	*26.48*	*38.89*	*34.29*
- *heavy oil*	*63.16*	*73.52*	*61.11*	*65.71*
Density (g/cm^3)	0.733	0.817	0.759	0.767
Total volume (cm^3)	1.30	3.95	4.85	4.95

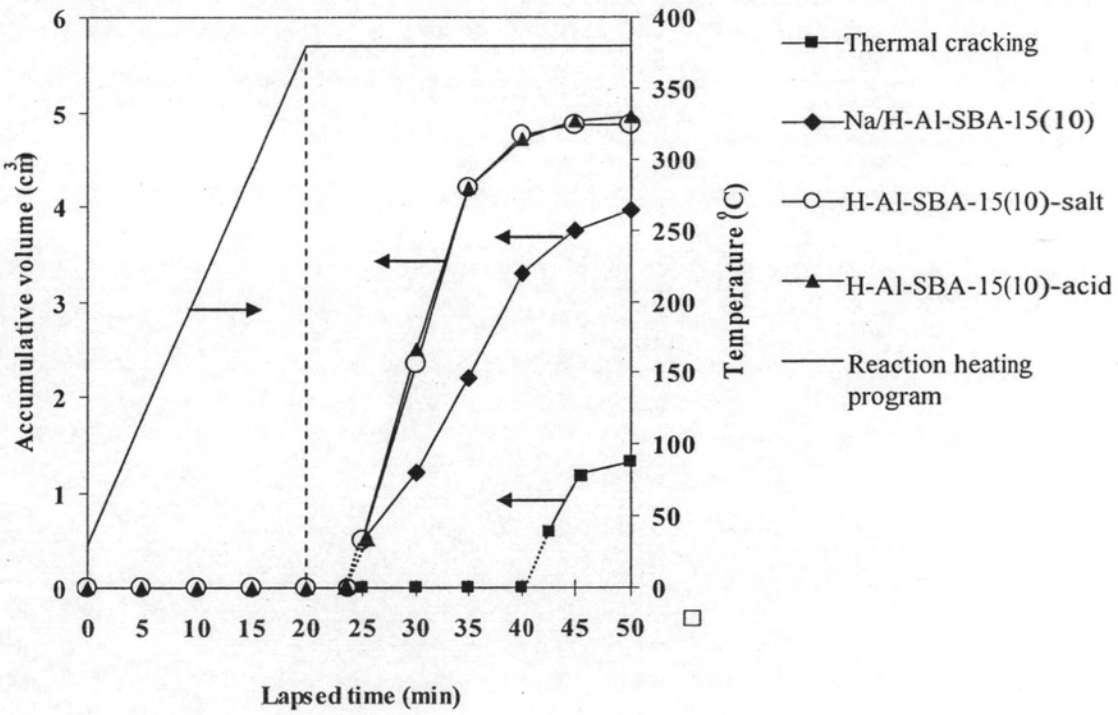

Figure 4.13 Accumulative volume of liquid fraction versus time for cracking of PP over SBA-15, and various Al-SBA-15(10) catalysts with different treatment at 380°C (Condition: 10%wt catalyst of PP, N_2 flow of 20 cm^3/min and reaction time of 30 min).

Gas product distribution from thermal cracking of PP over SBA-15 and various Al-SBA-15(10) catalysts is shown in Figure 4.14. Significant products selectivities to methane, propene, isobutene, n-pentane, and C5+ are found for thermal cracking at the values of 8, 29, 14, 14, and 12%, respectively. In the presence of SBA-15, the selectivities to these products changed to 9, 28, 6, 24, and 10%, respectively. In this work SBA-15 might absorb thermal energy, hence, reducing effective reaction temperature and the power of cracking and, as a result, no further conversion of n-pentane to isobutene. H-Al-SBA-15(10)-salt and H-Al-SBA-15(10)-acid provide the same product distribution in gas fraction with the high selectivities to methane, propene, iso-butene and C5+ group, *i.e.* 11, 17, 15, and 23%, approximately. The selectivity to n-pentane drastically decreases for all Al-SBA-15(10) catalysts. However, Na/H-Al-SBA-15(10) gives lower selectivity to iso-butene together with higher selectivity to methane, ethane, ethene and propane compared to fully acid H-Al-SBA-15(10)-acid and H-Al-SBA-15(10)-salt. This is due to the effect of sodium ions in Na/H-Al-SBA-15(10). Sodium ions reduced the acidity and occupied more space in the catalyst structure than H^+, resulting in different performance of the catalysts having the same structure but different amount of sodium ions.

Carbon number distribution of liquid fraction obtained by cracking of PP over SBA-15 and various Al-SBA-15(10) catalysts is shown in Figure 4.15. Liquid product is identified with the C_{np} value which relates to the boiling of normal-paraffins [47]. For example, the product in the range of C6 represent for a combination of some aliphatic, alicyclic, and aromatic hydrocarbon which have boiling points between those of n-pentane and n-hexane. For thermal cracking promotes the liquid product mainly in the range of C8-C9 hydrocarbons with C9 as the most predominant product group and it is absolutely different from that for the reaction in the presence of Al-SBA-15(10) catalysts. The profiles of liquid distribution obtained by cracking of PP over all Al-SBA-15(10) catalysts are approximately similar in the range of C6-C9 hydrocarbon with C7 and C8 as the most predominant groups. There is little different in % selectivity compared among these catalyst having the same structure due to the effects of sodium ions and the ion-exchange treatment.

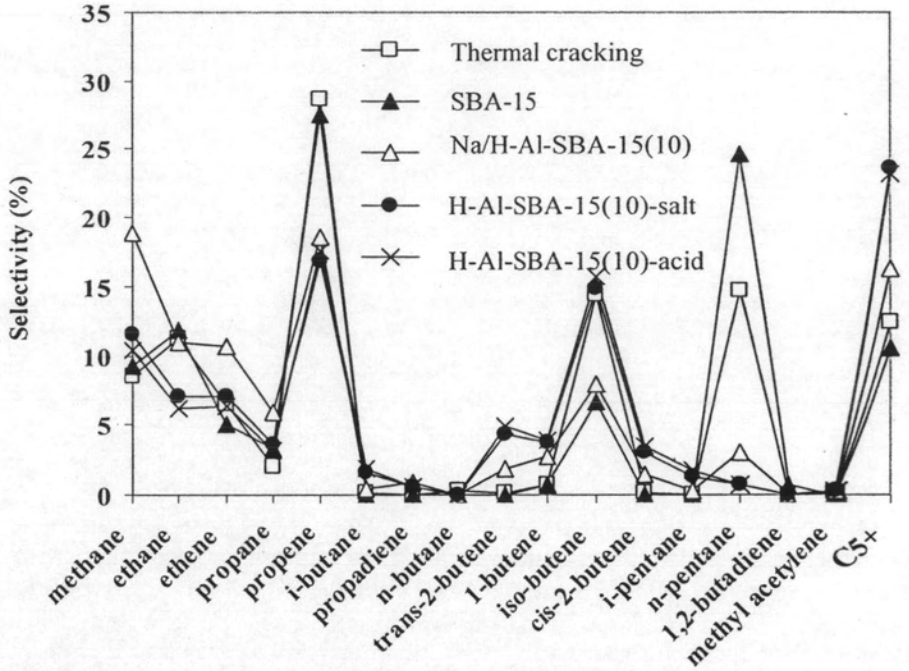

Figure 4.14 Gas product distributions from cracking of PP over SBA-15, and various Al-SBA-15(10) catalysts with different treatment at 380°C (Condition: 10%wt catalyst of PP, N_2 flow of 20 cm^3/min and reaction time of 30 min).

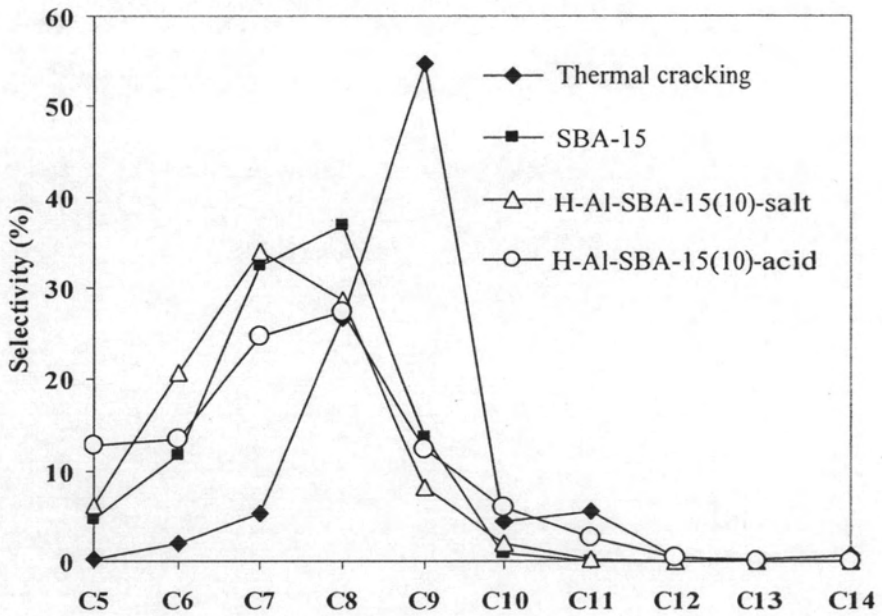

Figure 4.15 Carbon number distribution of liquid fraction obtained by cracking of PP over SBA-15, and various Al-SBA-15(10) catalysts with different treatment at 380°C (Condition: 10%wt catalyst of PP, N_2 flow of 20 cm^3/min and reaction time of 30 min).

It can be concluded that H-Al-SBA-15-acid and H-Al-SBA-15-salt behave similarly as catalyst in cracking of PP. However, H-Al-SBA-15-salt is the most proper catalyst to be applied in catalytic cracking of PP because HNO_3 is a harmful chemical, by generating the toxic gas (NO_x), and corrosive to apparatus. As a result, ion exchange of Al-SBA-15 with 0.01M NH_4Cl for 24 h is the most suitable procedure to be applied to catalytic cracking of PP in term of activity, product selectivity, safety and environment friendly. After this, the modified method will be use of 0.01 M NH_4Cl for ion exchange of Na/H-Al-SBA-15 prior to the use as catalyst.

4.3.2 Effect of reaction temperature

Values of conversion and product yield from catalytic cracking of PP over H-Al-SBA-15-(10)-salt at various temperatures of 360, 380 and 400°C are shown in Table 4.5. Conversion values of PP at the three temperatures are almost 100% with small amounts of residue. The activities of H-Al-SBA-15(10)-salt catalysts in cracking of PP are very high up to 97-98% even at the temperature of 360°C. The conversion is not significantly affected by the temperatures varied from 360-400°C due to only small difference in temperatures. For all cases, the products are mainly in liquid fraction at the yields above 71-73% with minor product in gas fraction at the yields abut 24-25%. The residue is varied from 2.00-3.00% with wax about 1.22-2.15% and solid coke about 0.6-0.8%.

Table 4.5 Conversion and product yield from catalytic cracking of PP over H-Al-SBA-15(10)-salt at various temperatures (Condition: 10%wt catalyst of PP, N_2 flow of 20 cm^3/min and reaction time of 30 min)

	Temperature		
	360°C	380°C	400°C
Conversion[a] (%)	97.20	97.00	98.00
Yield[b] (%)			
gas fraction	25.40	24.00	24.40
liquid fraction	71.80	73.00	73.60
residue	2.80	3.00	2.00
- wax	*2.12*	*2.15*	*1.22*
- solid coke	*0.68*	*0.85*	*0.78*

[a] *deviation within 0.45%*
[b] *deviation within 0.71%*

The properties of liquid fraction from cracking of PP over H-Al-SBA-15(10)-salt at various temperatures are shown in Table 4.6. Due to the insignificant difference in temperatures in the range of 360-380°C, the ratios of light oil and heavy oil in liquid fraction are not different. The only difference is the initial rate of liquid formation as interpreted from Figure 4.16 which shows the plots of accumulative volume of liquid fraction versus lapsed time for PP cracking over H-Al-SBA-15-salt (10) at various reaction temperatures. When the temperature is increased, the initial rate of liquid formation is faster. The rate of liquid formation is in the order of 400°C > 380°C > 360°C.

Table 4.6 Properties of liquid fraction from cracking of PP over H-Al-SBA-15(10)-salt at various temperatures (Condition: 10%wt catalyst of PP, N_2 flow of 20 cm^3/min and reaction time of 30 min)

Properties of liquid fraction	Temperature		
	360°C	380°C	400°C
Selectivity (%)			
-light oil	*35.80*	*38.89*	*36.67*
-heavy oil	*64.20*	*61.11*	*63.33*
Density (g/cm^3)	0.747	0.759	0.756
Total volume (cm^3)	4.50	4.85	5.00

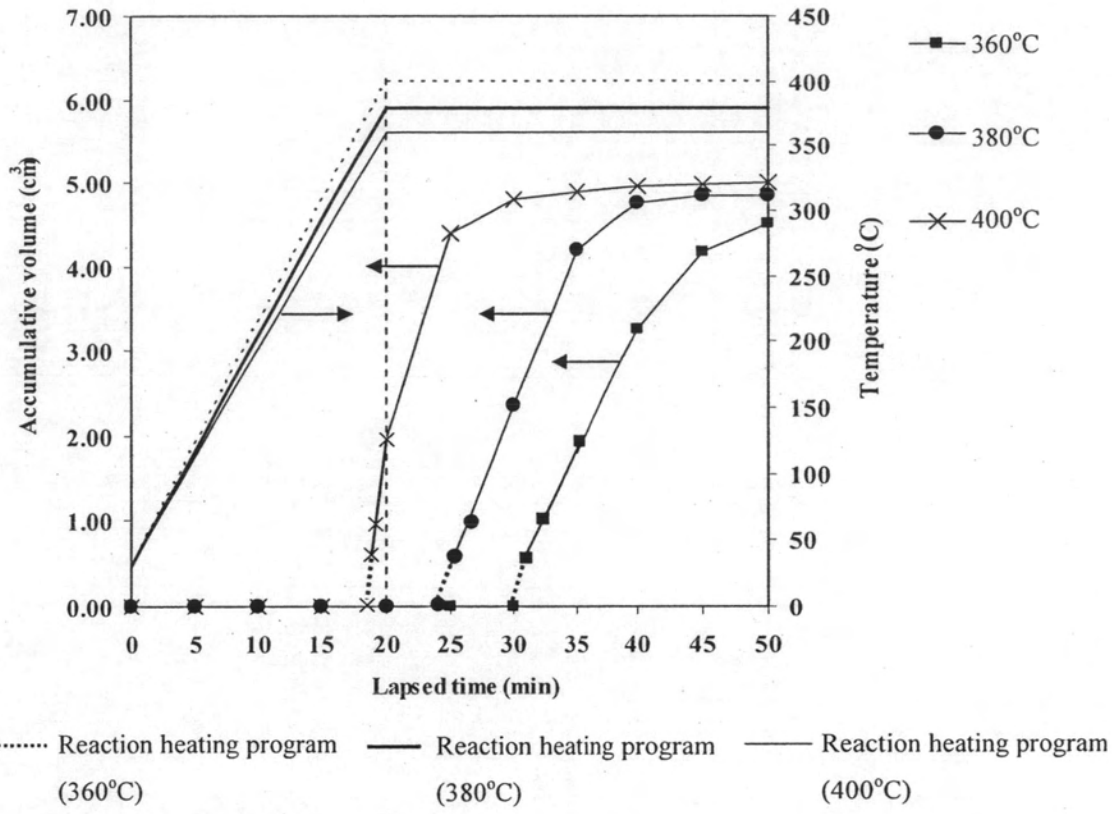

Figure 4.16 Accumulative volume of liquid fraction versus time for PP cracking over H-Al-SBA-15(10)-salt at various temperatures (Condition: 10%wt catalyst of PP, N_2 flow of 20 cm^3/min and reaction time of 30 min).

The gas product distributions from PP cracking catalyzed by H-Al-SBA-15 (10)-salt at various reaction temperatures are shown in Figure 4.17. There are not significantly different in distribution of gas fraction at the temperatures of 360, 380 and 400°C. Among gaseous products, formation of methane, propene, isobutene and C5+ are favored. Carbon number distribution of liquid fraction obtained by cracking of PP over H-Al-SBA-15(10)-salt at various temperatures is shown in Figure 4.18. The profiles of liquid distribution obtained by cracking of PP over all H-Al-SBA-15(10)-salt catalysts are in the range of C6-C9 hydrocarbon with C7 and C8 as the most predominant groups. It can not be mentioned about the temperature independence of the selectivities due to the insignificant difference in temperatures in the range of 360-380°C.

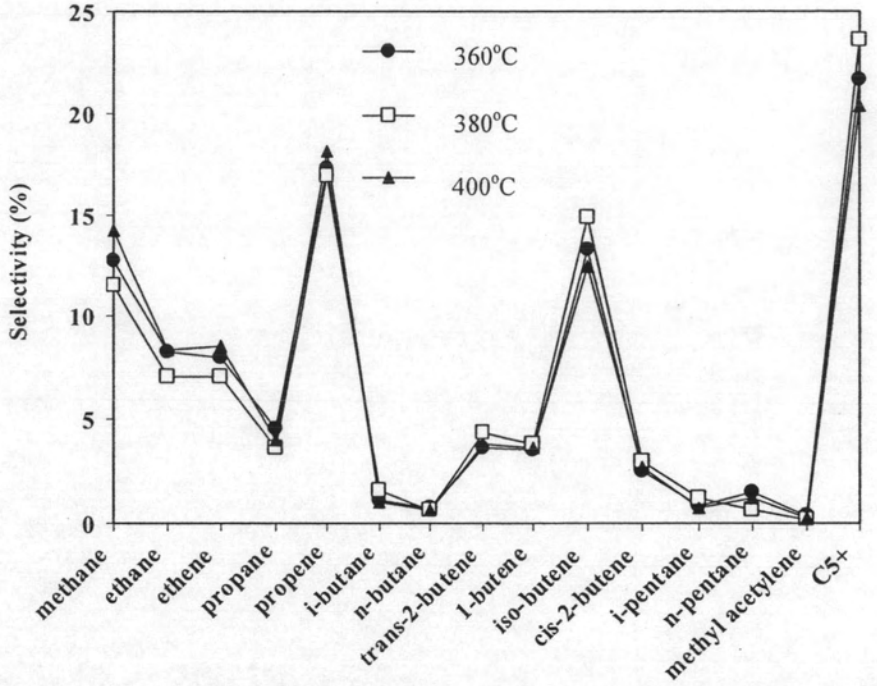

Figure 4.17 Gas product distributions from PP cracking catalyzed by H-Al-SBA-15-salt(10) at various temperatures (Condition: 10%wt catalyst of PP, N_2 flow of 20 cm^3/min and reaction time of 30 min).

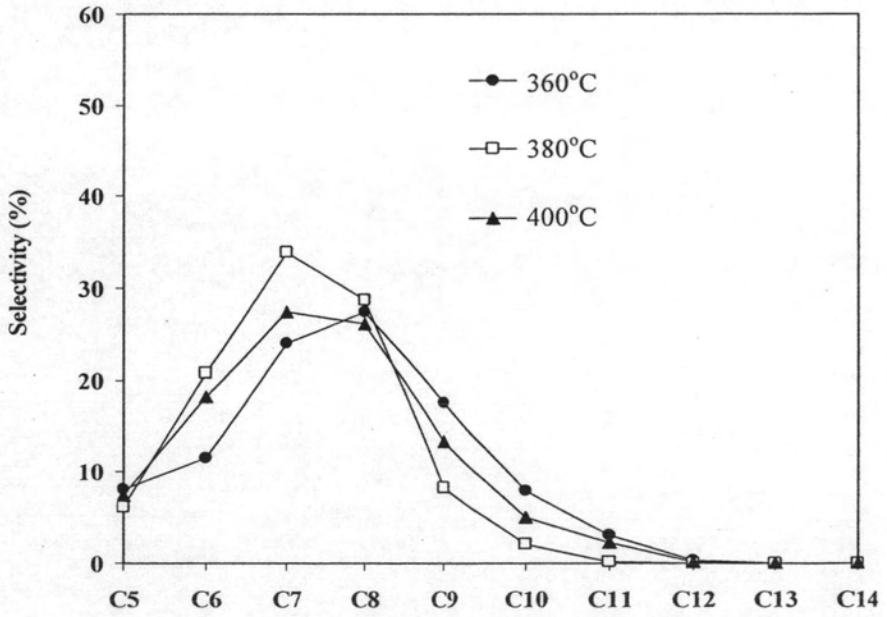

Figure 4.18 Carbon number distribution of liquid fraction obtained by PP cracking catalyzed by H-Al-SBA-15(10)-salt at various temperatures (Condition: 10%wt catalyst of PP, N_2 flow of 20 cm^3/min and reaction time of 30 min).

4.3.3 Effect of polypropylene to catalyst ratio

Values of conversion and product yield from PP cracking over H-Al-SBA-15(10)-salt at various catalyst amounts of 5 wt%, 10 wt%, and 15 wt% to PP are shown in Table 4.7. The same high conversion value of 97% are obtained in the cases of using 10 wt% and 15 wt% catalyst amounts but the conversion decreases to 83% in the case of using only 5% catalyst amount. The conversion strongly depends on the catalyst amount not exceeding 10%. However, the ratios of liquid fraction and gas fraction are different for 10% and 15% catalyst amounts. The excess amount of catalyst further makes the liquid fraction undergo cracking to smaller molecules in form of gas products. The amount of residue and the conversion are inversely related. The residue produced by using 5% catalyst amount contains mainly wax due to lower activity compared to the cases using larger amounts of catalyst. Similarly to previous discussion on other cases, the lower activity, the higher wax and residue is found.

Table 4.7 Conversion and product yield from PP cracking over H-Al-SBA-15(10)-salt at various catalyst amounts (Condition: N_2 flow of 20 cm^3/min, 380°C and reaction time of 30 min)

	Catalyst amount to PP		
	5 wt%	10 wt%	15 wt%
Conversion[a] (%)	83.60	97.00	97.00
Yield[b] (%)			
gas fraction	39.20	24.00	33.00
liquid fraction	44.40	73.00	64.00
residue	16.40	3.00	3.00
-wax	*14.10*	*2.15*	*2.44*
-solid coke	*2.30*	*0.85*	*0.56*

[a] *deviation within 0.45%*
[b] *deviation within 0.71%*

The selectivity to light oil and heavy oil in liquid fraction is affected by the catalysts amount. The higher amount of catalyst, the lower selectivity to light oil is obtained. The total volumes of liquid fraction indicate that the amount of 5% catalyst providing only 2.45 cm^3 that is not enough to make maximum volume of the liquid

fraction while the excess catalyst amount is not beneficial on increasing yield of liquid fraction more than 4.20 cm^3. The optimum catalyst amount is the 10 wt% catalyst to PP giving the greatest total volume of liquid fraction of 4.85 cm^3.

Table 4.8 Properties of liquid fraction from cracking of PP over H-Al-SBA-15(10)-salt at various catalyst amounts (Condition: N_2 flow of 20 cm^3/min, 380°C and reaction time of 30 min)

Properties of liquid fraction	Catalyst amount to PP		
	5 wt%	10 wt%	15 wt%
Selectivity (%)			
- *light oil*	*50.00*	*38.89*	*31.77*
- *heavy oil*	*50.00*	*61.11*	*68.23*
Density (g/cm^3)	0.88	0.76	0.75
Total volume (cm^3)	2.45	4.85	4.20

Figure 4.19 shows the kinetic rate in catalytic cracking of virgin PP beads over various amounts of H-Al-SBA-15(10)-salt. Comparing to the kinetic rate in the reaction using 10 wt% and 15 wt% catalyst amounts, it reveals the same kinetic rate of liquid formation from PP cracking. Upon prolongation of reaction using the 15% catalyst amount, the slope is different from the first interval, indicating the predominant competitive rate of dissociation of liquid molecules to gas molecules compared to the rate of liquid formation. As a result, the total of liquid fraction in the case of 15% catalyst amount is relatively less than that in the case of 10% catalyst amount.

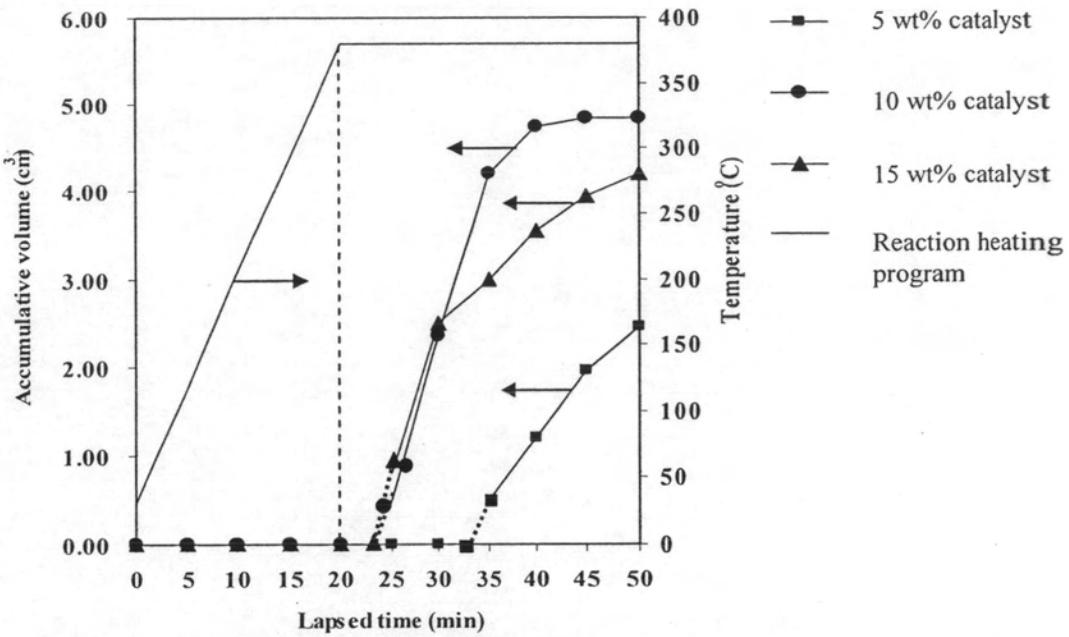

Figure 4.19 Accumulative volume of liquid fraction versus time for PP cracking over H-Al-SBA-15(10)-salt at various catalyst amounts (Condition: N_2 flow of 20 cm^3/min, 380°C and reaction time of 30 min).

Gas and liquid product distribution from PP cracking catalyzed by H-Al-SBA-15(10)-salt at various catalyst amounts are presented in Figure 4.20 and 4.21, respectively. The favored gaseous products are methane, propene, isobutene and C5+. The selectivity of gas fraction for 5% and 15% catalyst amounts are similar but different from that for the 10% catalyst amount. Using the 5% catalyst amount favors heavy C8-C9 group due to the catalyst amount is not enough to complete cracking of heavy molecules. Using the 10% catalyst amount provides the favored products of trans-2-butene and isobutene in gas fraction and also C6-C8 groups in liquid fraction. Surprisingly, increasing to 15% catalyst amount the selectivity to each liquid component in liquid fraction seems to be between the cases of 5 and 10% catalyst amounts while the selectivity in gas fraction is close to the case 5% rather than 10% catalyst amount. It can be explained by the effect of catalyst amount but the relation is not in sequence due to the very wide range of varied values. It may be in sequence in a specific range of catalyst amount less than 10%. Thus the wide range distribution of product depends on the catalyst amount, the choice depends on what type of product is required. In this work, the choice is using 10% catalyst amount according to the fastest rate of liquid formation and the highest yield of liquid fraction.

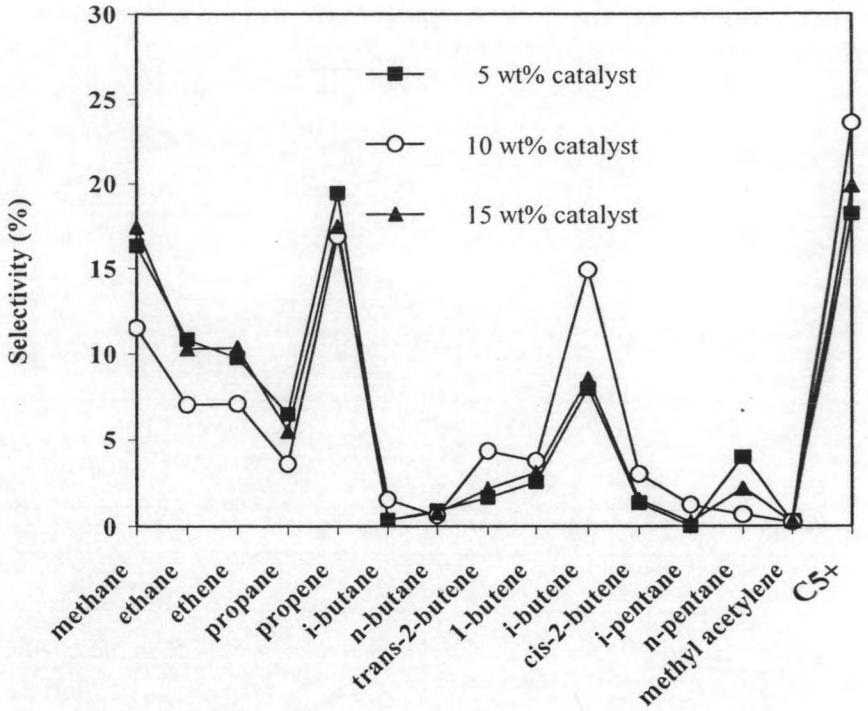

Figure 4.20 Gas product distribution from PP cracking catalyzed by of H-Al-SBA-15(10)-salt at various catalyst amounts (Condition: N_2 flow of 20 cm^3/min, 380°C and reaction time of 30 min).

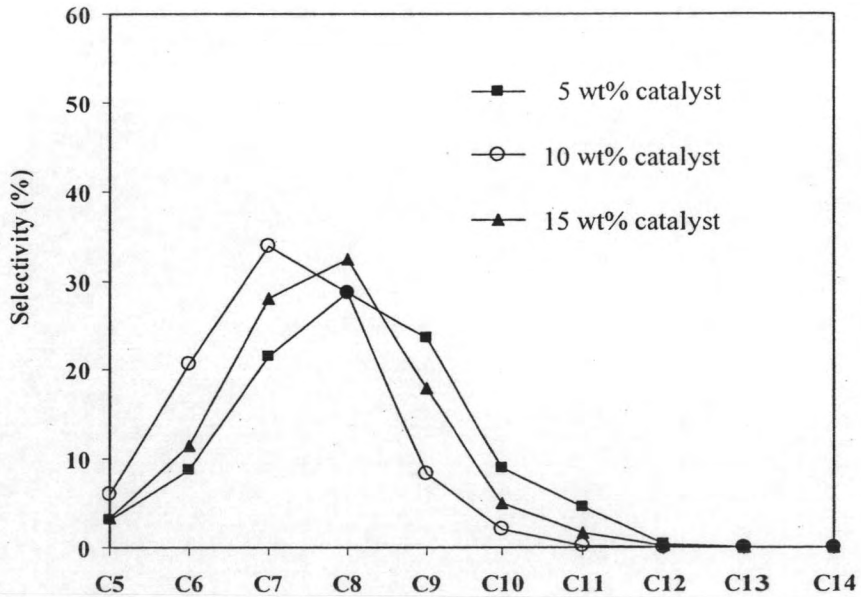

Figure 4.21 Carbon number distribution of liquid fraction obtained by PP cracking catalyzed by H-Al-SBA-15(10)-salt at various catalyst amounts (Condition: N_2 flow of 20 cm^3/min, 380°C and reaction time of 30 min).

4.3.4 Effect of aluminum content in catalyst

Conversion and product yield from PP cracking over H-Al-SBA-15-salt with various Si/Al ratios are shown in Table 4.9. The properties of liquid fraction from cracking of PP over H-Al-SBA-15-salt at various Si/Al ratios in catalyst are shown in Table 4.10. Basically, the higher Si/Al ratio or lower Al content, the lower acidity of the catalyst is, and at the same time the higher surface area is. It is known that the activity would decrease with decreasing acidity and surface area. From Table 4.9, the conversions ranging form 96.80 to 98.20% seem to be independent from the Si/Al ratios in catalyst and the BET specific surface areas. The synergism of catalyst surface area and acidity of H-Al-SBA-15 contributed to the PP conversion in the cracking process. The decrease in lower conversion is compensated by the increase in BET specific surface area. As a result, the conversions are not much different for all Si/Al ratios in catalyst. However, by increasing the Si/Al ratio in catalyst the yield in gas fraction slightly increases while the yield in liquid fraction decreases due to the predominant effect of specific surface area over the effect of acidity causing the cracking of liquid fraction to gas fraction.

The lower acidity of H-Al-SBA-15-salt (100) compared with other catalysts results in the formation of heavier liquid product and this fraction causes the overall yield to increase. The selectivity to heavy oil fraction are found to have an opposite trend to light oil fraction, indicating that the effect of secondary cracking reaction plays the role for production of light oil fraction. The combined effects of acidity and surface area account for the irregular order of selectivities to light oil and heavy oil based on the Si/Al ratios in catalyst.

The plots of accumulative volume of liquid fraction versus lapsed time for PP cracking over H-Al-SBA-15-salt with various Si/Al ratios are shown in Figure 4.22. At the beginning there is no significant difference between rates of liquid formation catalyzed by these catalysts. The catalyst with Si/Al ratio of 100 is obviously slower than the one with Si/Al ratio of 10 after prolongation of the reaction for a while. Therefore, the total volumes of these two catalysts are different. This is not due to the effect of surface area but the effect of acidity of catalyst or Si/Al ratio in catalyst.

Table 4.9 Conversion and product yield from PP cracking over H-Al-SBA-15-salt with various Si/Al ratios (Condition: 10%wt catalyst of PP, N_2 flow of 20 cm^3/min, 380°C and reaction time of 30 min)

	Si/Al ratio in catalyst				
	(10)	(15)	(30)	(50)	(100)
BET specific surface area (m^2/g)	440	505	571	603	613
Conversion[a] (%)	97.00	96.80	96.80	97.40	98.20
Yield[a] (%)					
gas fraction	24.00	25.80	26.40	29.40	30.80
liquid fraction	73.00	71.00	70.40	68.00	67.40
residue	3.00	*3.20*	3.20	2.60	1.80
- wax	*2.15*	*2.35*	*2.38*	*2.05*	*1.24*
- solid coke	*0.85*	*0.85*	*0.82*	*0.55*	*0.56*

[a] Deviation within 0.60%

Table 4.10 Properties of liquid fraction from cracking of PP over H-Al-SBA-15(10)-salt at various Si/Al ratios in catalyst (Condition: 10%wt catalyst of PP, N_2 flow of 20 cm^3/min, 380°C and reaction time of 30 min)

Properties of liquid fraction	Si/Al ratio in catalyst				
	(10)	(15)	(30)	(50)	(100)
Selectivity (%)					
- light oil	*38.89*	*42.01*	*43.79*	*38.96*	*36.32*
- heavy oil	*61.11*	*57.99*	*56.21*	*61.04*	*63.68*
Density (g/cm^3)	0.759	0.755	0.740	0.745	0.732
Total volume (cm^3)	4.85	4.80	4.70	4.60	4.55

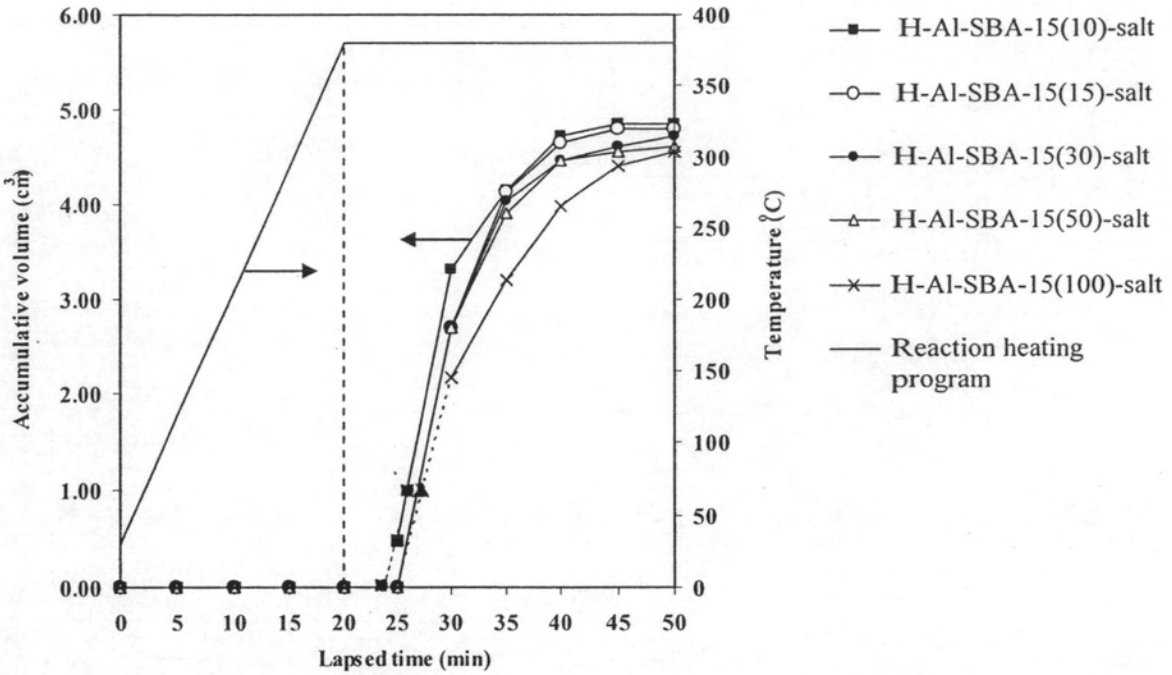

Figure 4.22 Accumulative volume of liquid fraction versus time for PP cracking over H-Al-SBA-15-salt with various Si/Al ratios (Condition: 10%wt catalyst of PP, N_2 flow of 20 cm^3/min, 380°C and reaction time of 30 min).

The profiles of gas product distribution from PP cracking catalyzed by H-Al-SBA-15-salt with various Si/Al ratios are shown in Figure 4.23. The profiles of gas product distribution are almost not different when changing the Si/Al ratio in catalyst except in the region of C1-C2 hydrocarbons. Only the one with Si/Al ratio of 15 looks different from others. As mentioned earlier of this section that both effects of acidity and specific surface area play important roles on the performance of catalysts with different Si/Al ratios. These effects make difficulties in explanation of the results. However, all are in agreement with the fact that the decrease in amount of heavier components causes the decrease in amount of lighter components in both gas and liquid fractions.

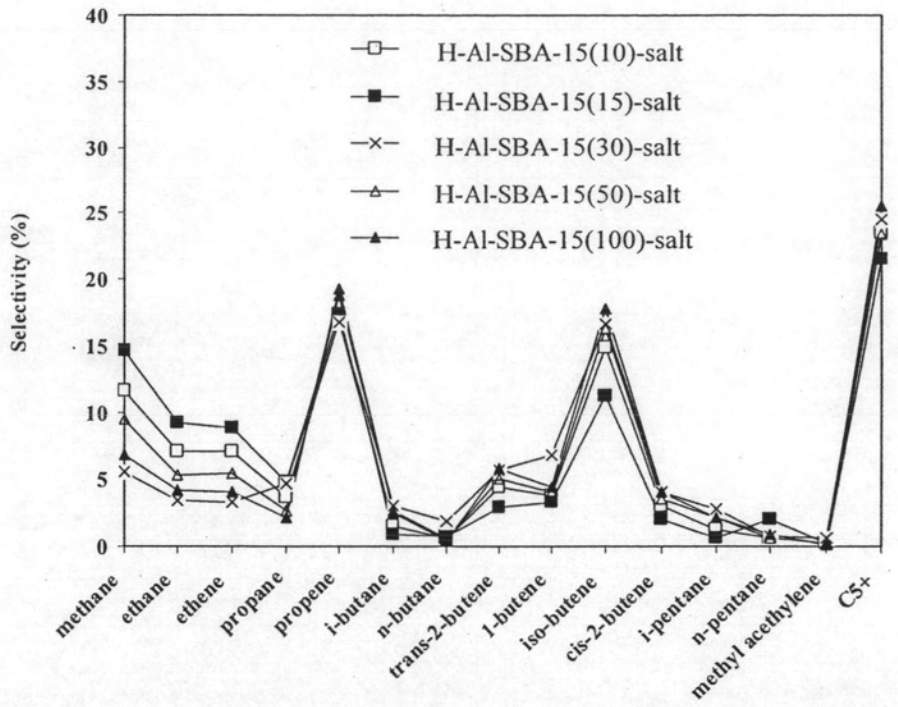

Figure 4.23 Gas product distribution from PP cracking catalyzed by H-Al-SBA-15-salt with various Si/Al ratios (Condition: 10%wt catalyst of PP, N_2 flow of 20 cm^3/min, 380°C and reaction time of 30 min).

In liquid fraction the product distribution profiles are almost the same for all catalysts except the one with Si/Al of 100 having higher selectivity to C9 but lower selectivity to C6 due to its lowest acidity compared to others. However, all catalysts provide the similar high selectivity to C7and C8.

By comparing with standard gasoline distribution as shown in Figure 4.25, it is found that the major components in commercial gasoline are in the range of C7-C8. Hence, it can be concluded that H-Al-SBA-15-salt catalysts with Si/Al ratios 10-100 can be the good cracking catalysts for conversion PP to the valuable fraction of liquid hydrocarbon in the range of gasoline.

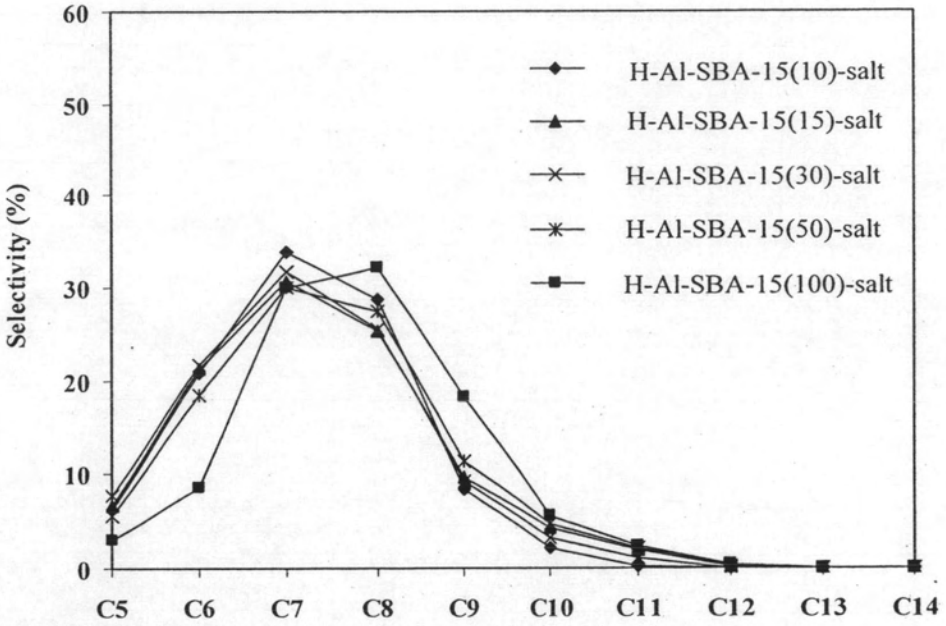

Figure 4.24 Carbon number distribution of liquid fraction obtained by PP cracking catalyzed by H-Al-SBA-15-salt with various Si/Al ratios (Condition: 10%wt catalyst of PP, N_2 flow of 20 cm^3/min, 380°C and reaction time of 30 min).

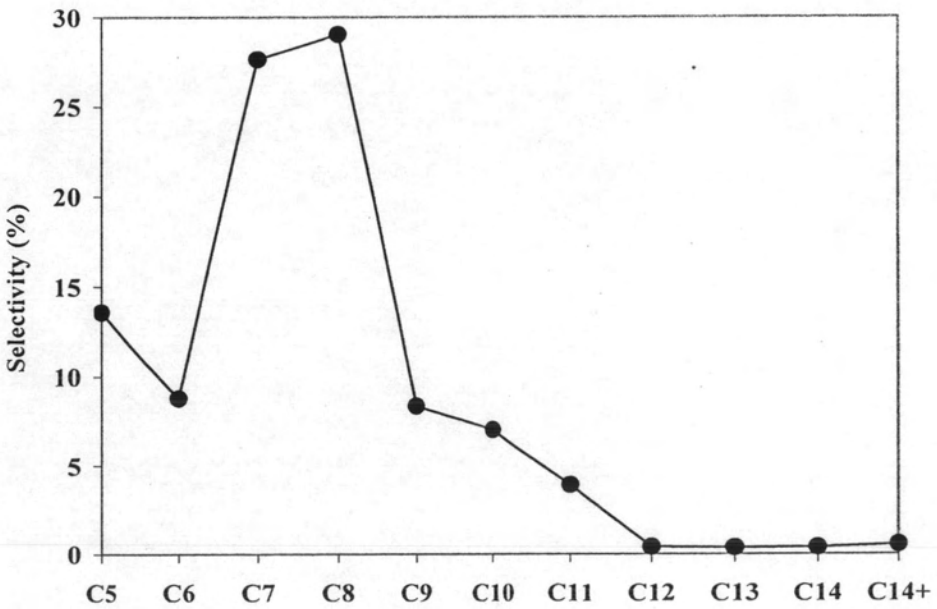

Figure 4.25 Distribution of components in standard gasoline (SUPELCO).

4.4 Recycle of catalyst

4.4.1 Characterization of regenerated and spent catalysts

Many researchers claimed that the higher the aluminum content, the easier the structure deterioration is; therefore, in this work the spent H-Al-SBA-15(10)-salt catalyst has been reused with and without regeneration in cracking of PP. The used catalyst was washed with hexane for several times and then dried at 125°C for 3 h; it is denoted as spent H-Al-SBA-15(10)-salt. The regenerated catalyst refers to the spent catalyst calcined at 550°C for 5 h in order to remove the solid coke from the catalyst pores. It is denoted as regen-H-Al-SBA-15(10)-salt. All recycled catalysts are characterized by XRD technique and surface area analysis. Figure 4.29 shows the XRD patterns of the recycled catalysts, confirmed that the regenerated and the spent catalysts still exhibit a characteristic XRD patterns like the fresh one. The spent catalyst has the lowest (100) reflection peak intensity due to partial damage of structure during cracking reaction but the catalyst structure was able to be recovered by calcination, *i. e.* structure re-engineering. The peak intensity of the regenerated catalyst decreases because the catalyst structure was partially destroyed during reaction and regeneration via coke burning at elevated temperature (550°C) and cannot recur fully. The adsorption-desorption isotherms of those catalysts are presented in Figure 4.30. The regenerated catalyst shows the characteristic isotherm of mesoporous materials with the specific surface area of 413 m^2/g that was slightly reduced by 6% as compared to the fresh one (440 m^2/g).

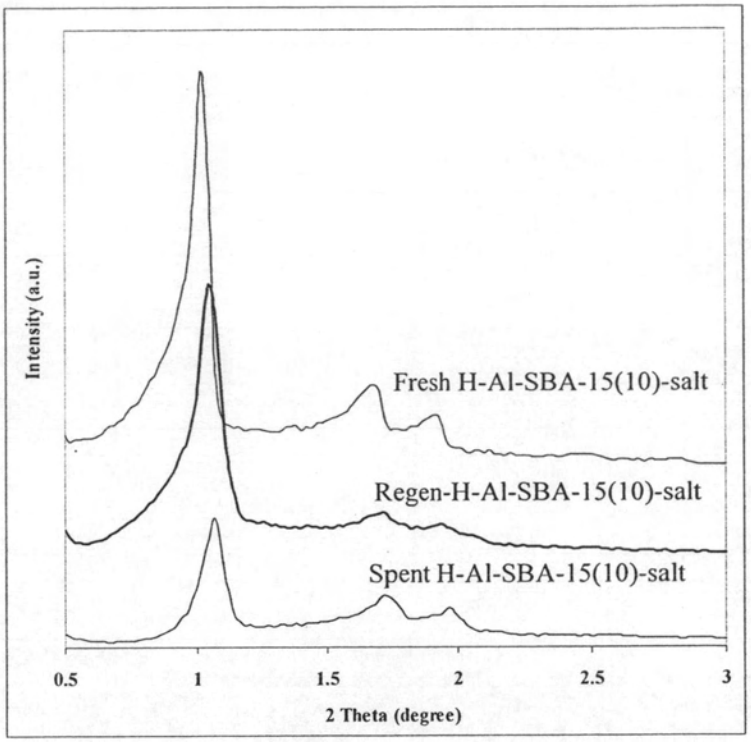

Figure 4.26 XRD patterns of fresh, regenerated and spent H-Al-SBA-15(10)-salt catalysts.

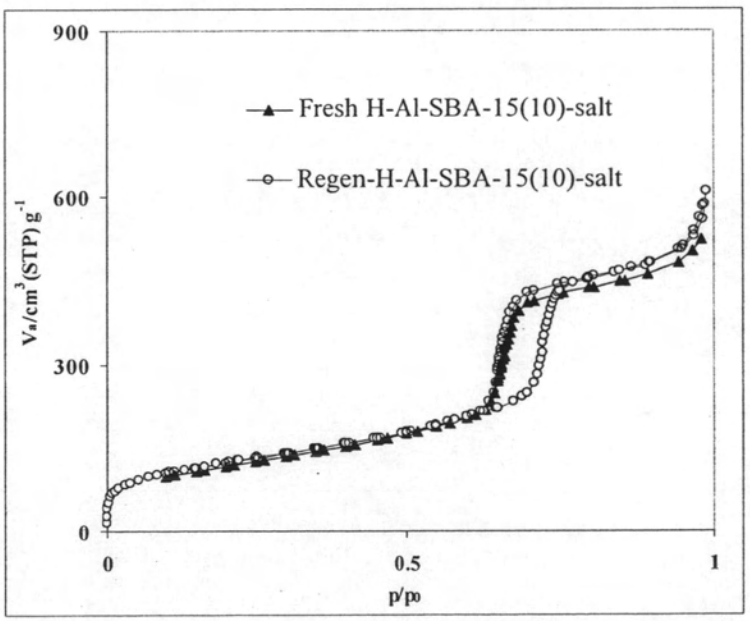

Figure 4.27 N_2 adsorption-desorption isotherms of fresh and regenerated H-Al-SBA-15(10)-salt catalysts.

4.4.2 Activity of regenerated and spent catalysts

The catalytic cracking of PP has been carried out at the optimum condition (reaction temperature of 380°C for 30 min) with 10 wt% catalyst. The values of conversion and product yield obtained are shown in Table 4.8.

Table 4.11 Conversion and product yield from PP cracking over fresh, regenerated and spent H-Al-SBA-15(10)-salt catalysts (Condition: 10%wt catalyst of PP, N_2 flow of 20 cm^3/min, 380°C and reaction time of 30 min)

	Fresh H-Al-SBA-15(10)-salt	Regen-H-Al-SBA-15(10)-salt	Spent H-Al-SBA-15(10)-salt
BET specific surface area (m^2/g)	440.99	412.67	-
Conversion[a] (%)	97.00	96.60	98.40
Yield[b] (%)			
gas fraction	24.00	22.00	29.00
liquid fraction	73.00	74.60	69.40
residue	3.00	3.40	1.60
- wax	*2.15*	*3.17*	*1.09*
- solid coke	*0.85*	*0.23*	*0.51*

[a] Deviation within 0.45%

[b] Deviation within 0.71%

From Table 4.11, very high conversion values above 96.60% are still obtained with regenerated catalyst and 98.40% with spent catalyst. There is no doubt about regenerated catalyst having almost the same conversion of PP. As compared to the fresh catalyst, the yield of gas fraction obtained for the regenerated catalyst is relatively higher while the yield of liquid fraction is relatively lower due to the relatively less specific surface area. However, slightly higher conversion for the unregenerated spent catalyst than that for the fresh catalyst is unexpected. It implies that liquid oil was not totally removed from the pores of used catalyst upon washing with n-hexane due to the very high surface area of catalyst resulting high adsorptive property. When it was reused, the oil just readily underwent re-cracking giving higher conversion and gas fraction than the actual amounts [52].

Properties of liquid fraction from cracking of PP over recycled H-Al-SBA-15(10)-salt catalysts are shown in Table 4.12. The selectivity to light oil is less than that to heavy oil for all cases. The selectivity to light oil decreases in the order for fresh catalyst > regenerated catalyst > spent catalyst and this is in agreement with the selectivity to heavy oil which is in the opposite order. The total volume of liquid fraction is about the same for the fresh and the regenerated catalysts while lower volume is obtained for the spent catalyst. The rate for liquid formation is comparable for the fresh and the regenerated catalysts but is reduced for the spent catalyst as shown in Figure 4.28. The results lead to the conclusion that the calcination process is needed in case of H-Al-SBA-15 catalyst.

Table 4.12 Properties of liquid fraction from cracking of PP over recycled H-Al-SBA-15(10)-salt catalysts (Condition: 10%wt catalyst of PP, 380°C, N_2 flow of 20 cm^3/min and reaction time of 30 min)

Properties of liquid fraction	Fresh H-Al-SBA-15(10)-salt	Regen-H-Al-SBA-15(10)-salt	Spent H-Al-SBA-15(10)-salt
Selectivity (%)			
-light oil	*38.89*	*35.24*	*33.86*
-heavy oil	*61.11*	*64.76*	*66.14*
Density (g/cm^3)	0.759	0.746	0.763
Total volume (cm^3)	4.85	4.90	4.50

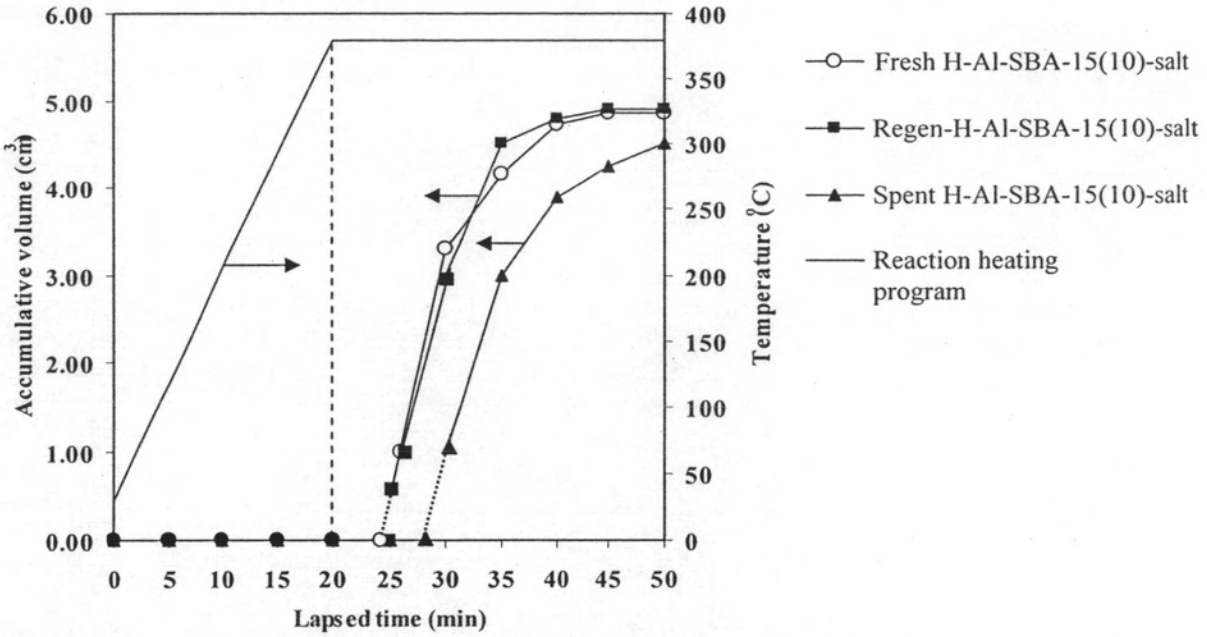

Figure 4.28 Accumulative volume of liquid fraction versus time for PP cracking over fresh, regenerated and spent H-Al-SBA-15(10)-salt (Condition: 10%wt catalyst of PP, N_2 flow of 20 cm^3/min, 380°C and reaction time of 30 min).

The profiles of gas product distribution from PP cracking over fresh, regenerated and spent H-Al-SBA-15(10) are shown in Figure 4.29. These results are similar to each other with major gaseous product as methane, propene, isobutene, and C5+. The spent catalyst provides higher selectivity to methane and lower selectivity to isobutene and C5+ than the fresh and the regenerated catalysts. The liquid product distributions are shown in Figure 4.33. The favored liquid products for the regenerated and the spent catalysts are still C7 and C8 groups with slightly decreasing selectivities as compared to the fresh catalyst. Selectivity to C9 only slightly increases for the recycled catalysts.

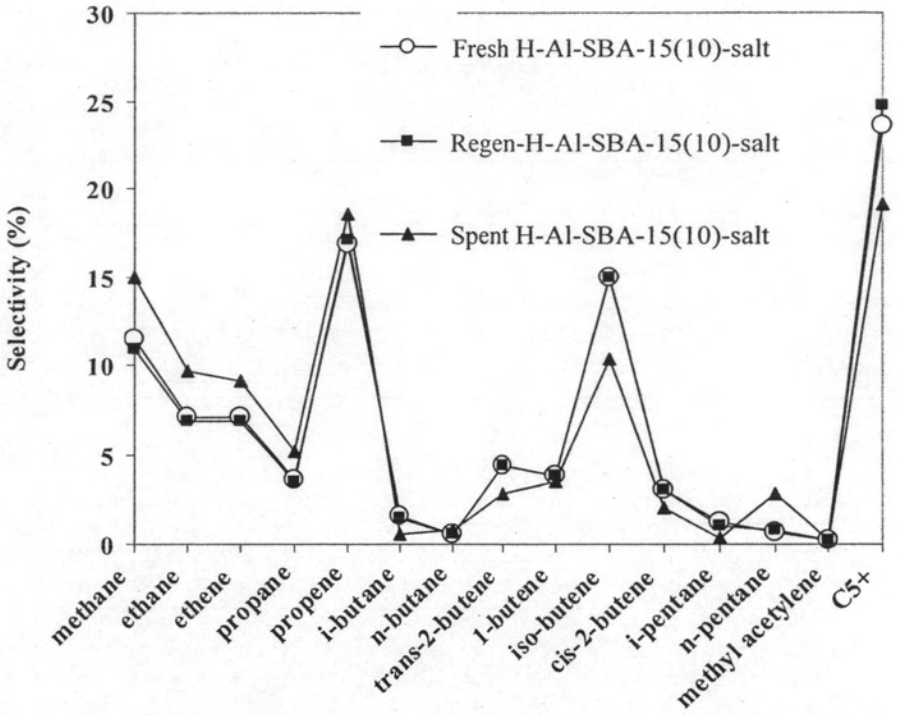

Figure 4.29 Gas product distribution from PP cracking over fresh, regenerated and spent H-Al-SBA-15(10)-salt (Condition: 10%wt catalyst of PP, N_2 flow of 20 cm^3/min, 380°C and reaction time of 30 min).

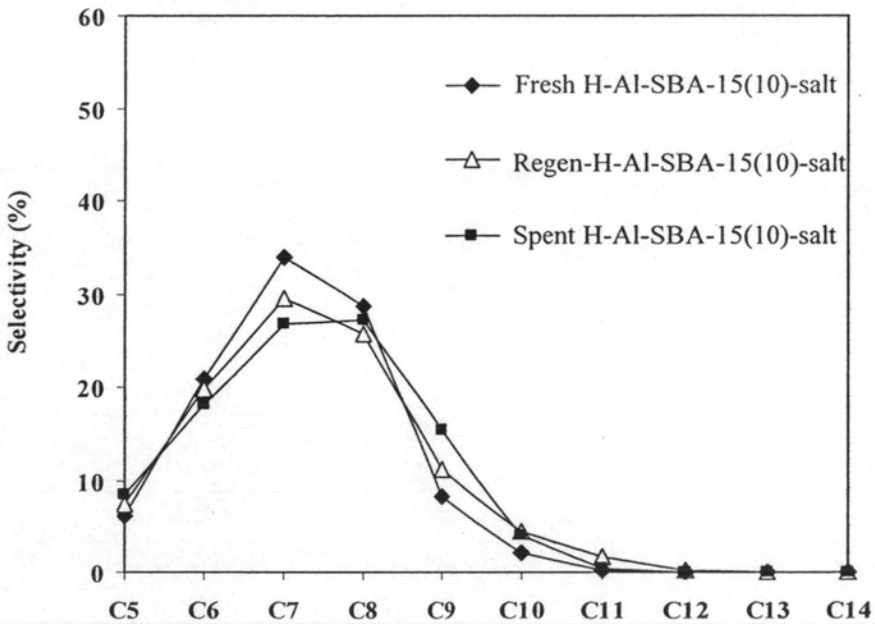

Figure 4.30 Carbon number distribution of liquid fraction obtained by PP cracking over fresh, regenerated and spent H-Al-SBA-15(10)-salt (Condition: 10%wt catalyst of PP, N_2 flow of 20 cm^3/min, 380°C and reaction time of 30 min).

4.5 Catalytic activity of H-Al-SBA-15 in polypropylene waste cracking

Conversion and product yield from PP waste cracking compared with PP beads cracking over H-Al-SBA-15(10)-salt and H-Al-SBA-15(30)-salt are shown in Table 4.13. There is no significant difference in overall performance. This proves that the catalysts used in this work can be applied to conversion of PP waste to gas and liquid fractions both of which can be used as alternative fuels. The properties of liquid fraction as shown in Table 4.14 indicate similar rate of liquid formation for cracking of PP bead and PP waste over H-Al-SBA-15(10)-salt. When H-Al-SBA-15(30)-salt was used as catalyst, the difference in rate of liquid formation for cracking of PP bead and PP waste is more obvious. The rate of liquid formation for cracking of PP bead is faster than that for PP waste. It implies that the difference may be more significant when less active catalyst is used. This can be explained by the effect of additives in plastic waste. In plastic shaping process, many additives, *i. e.* anti-oxidant, lubricating agent, pigment, *etc.* are used in order to improve the plastic properties and promote the easier processing of plastic, thus the additives can also promote the catalytic cracking of plastic to gas product. Moreover, as compared with virgin plastic cracking, plastic waste cracking provides higher proportion of heavy oil fraction.

Table 4.13 Conversion and product yield from PP waste cracking compared with PP beads cracking over H-Al-SBA-15(10)-salt and H-Al-SBA-15(30)-salt (Condition: 10%wt catalyst of PP, N_2 flow of 20 cm^3/min, 380°C and reaction time of 30 min)

	H-Al-SBA-15(10)-salt		H-Al-SBA-15(30)-salt	
	PP beads	PP waste	PP beads	PP waste
Conversion[a] (%)	97.00	96.60	96.80	95.40
Yield[a] (%)				
gas fraction	24.00	25.60	26.40	31.00
liquid fraction	73.00	71.00	70.40	64.40
residue	3.00	3.40	3.20	4.60
- wax	*2.15*	*2.37*	*2.38*	*3.63*
- solid coke	*0.85*	*1.03*	*0.82*	*0.97*

[a] Deviation within 0.60%

Table 4.14 Properties of liquid fraction from PP waste cracking compared with PP beads cracking over H-Al-SBA-15(10)-salt and H-Al-SBA-15(30)-salt (Condition: 10%wt catalyst of PP, N_2 flow of 20 cm^3/min, 380°C and reaction time of 30 min)

Properties of liquid fraction	H-Al-SBA-15(10)-salt		H-Al-SBA-15(30)-salt	
	PP beads	PP waste	PP beads	PP waste
Selectivity (%)				
- light oil	*38.89*	*36.83*	*43.79*	*40.53*
- heavy oil	*61.11*	*63.17*	*56.21*	*59.47*
Density (g/cm^3)	0.759	0.758	0.740	0.740
Total volume (cm^3)	4.85	4.80	4.70	4.30

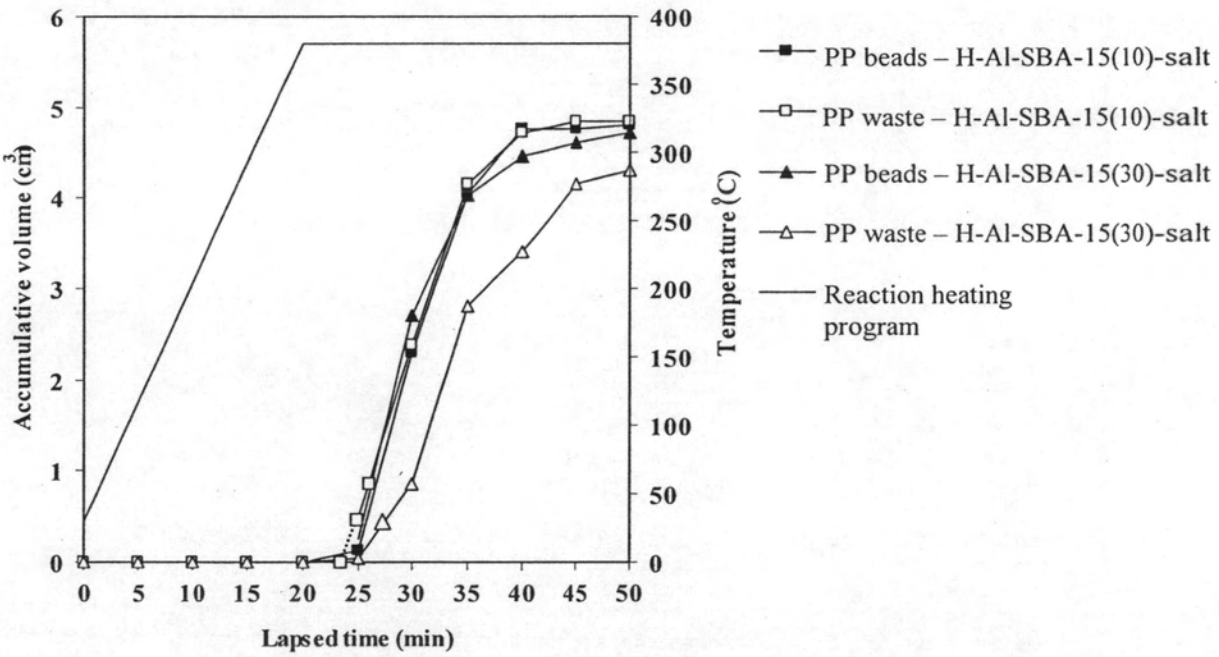

Figure 4.31 Accumulative volume of liquid fraction versus time for waste PP cracking compared with virgin PP cracking over H-Al-SBA-15(10)-salt and H-Al-SBA-15(30)-salt (Condition: 10%wt catalyst of PP, N_2 flow of 20 cm^3/min, 380°C and reaction time of 30 min).

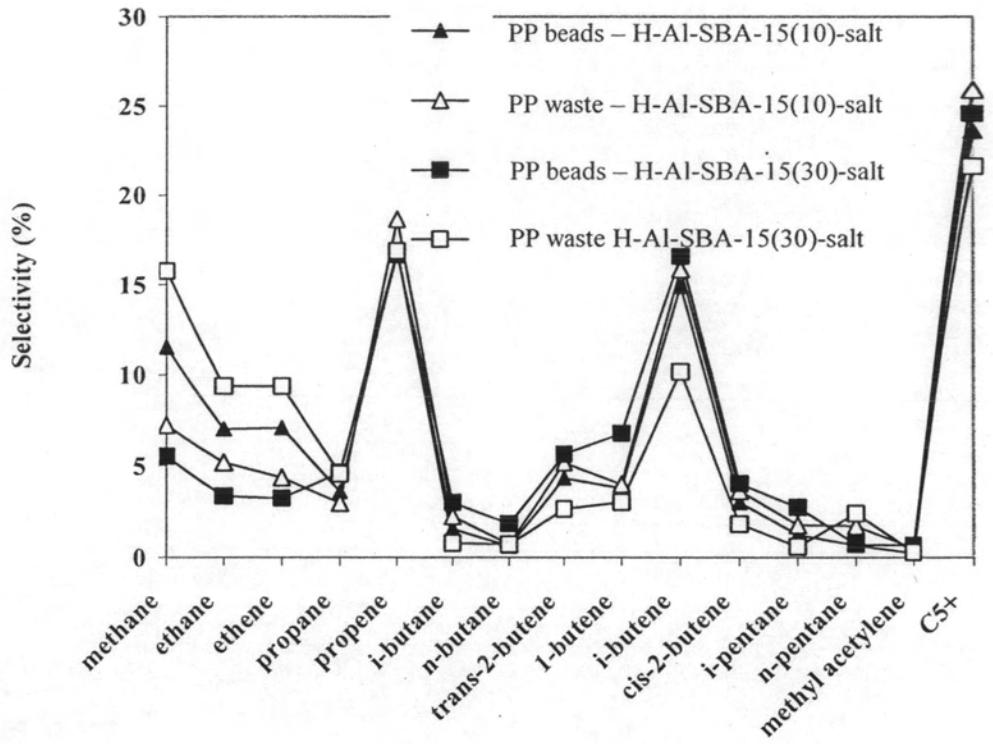

Figure 4.32 Gas product distribution from PP waste cracking compared with virgin PP cracking over H-Al-SBA-15(10)-salt and H-Al-SBA-15(30)-salt (Condition: 10%wt catalyst of PP, N_2 flow of 20 cm^3/min, 380°C and reaction time of 30 min).

Figure 4.32 exhibits the gas product composition obtained from PP waste cracking over H-Al-SBA-15(10)-salt and H-Al-SBA-15(30)-salt at the same condition to compare with cracking products from PP beads. All cases produce similar gas product distribution with the favored products of propene, isobutene and methane. Obviously, cracking of PP waste by H-Al-SBA-15(30)-salt provides lower isobutene and higher methane different from other cases. The cause of difference is rather complicate due to the additives in PP waste but not present in PP beads, and the competition between high surface area and low acidity of H-Al-SBA-15(30)-salt. The liquid product distribution of each reaction is revealed in Figure 4.33. It is obvious that the liquid products obtained in all cases have similar carbon number distribution which is in the same range of gasoline distribution as shown in Figure 4.25.

From the overall data, conversion, liquid formation rate and product distribution, H-Al-SBA-15-salt exhibits high activity in catalytic cracking of PP waste and high product selectivity to liquid product in the same range as that of standard

gasoline based on n-paraffin distribution. As a result, it can be concluded that H-Al-SBA-15 (with the Si/Al molar ratios of 10 and 30) are promising to be a very active catalyst in catalytic cracking of not only polypropylene beads but also polypropylene waste.

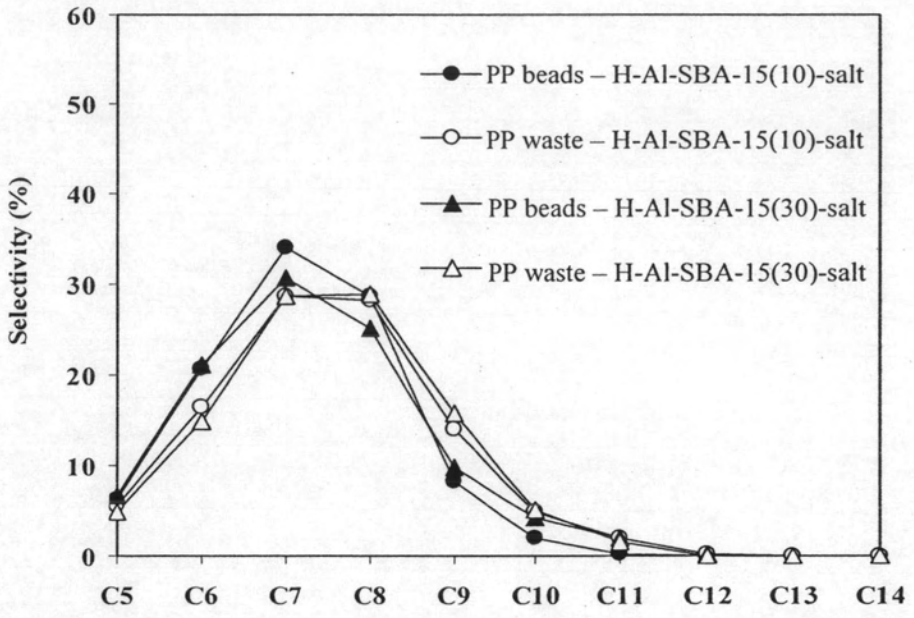

Figure 4.33 Carbon number distribution of liquid fraction obtained by PP waste cracking compared with virgin PP cracking over H-Al-SBA-15(10)-salt and H-Al-SBA-15(30)-salt (Condition: 10%wt catalyst of PP, N_2 flow of 20 cm^3/min, 380°C and reaction time of 30 min).

4.6 Proposed mechanism for catalytic cracking of PP over H-Al-SBA-15

The proposed mechanism for plastic cracking over heterogeneous catalyst has been carried out by Ishihara *et al.* [40] and Makkee *et al.* [51]. The most important elementary reactions are β-scission and intramolecular rearrangement of chain-end secondary carbonium ions in the liquid fraction to inner tertiary carbon atoms.

4.6.1 Generation of carbocation

In catalytic cracking of plastic, the following mechanism illustrates the different ways by which carbocations may be generated in the reactor:

1. Abstraction of a hydride ion from a hydrocarbon by a Lewis acid site of catalyst

2. Addition of a Brønsted acid site (H^+) in catalyst to olefin

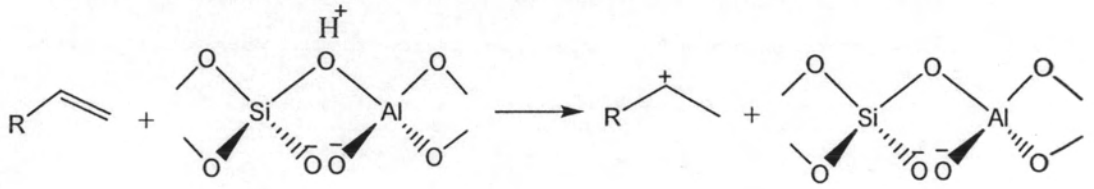

where R represents for polymer chain which has two end-chain types:

(A) (B)

4.6.2 Molecular weight reduction through β-scission

Cracking of the adsorbed carbocation takes place through β-scission mechanism. Propene and isobutene as major gaseous product may be produced as follows:

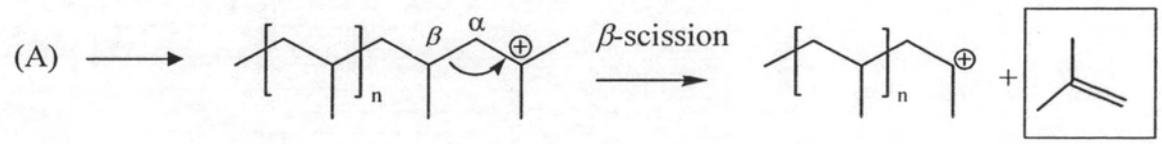

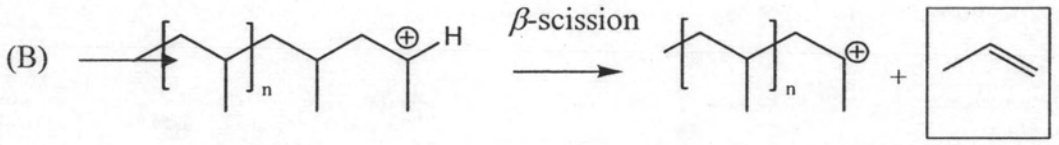

Carbocation can rearrange through a methide-hydride shift to the stable form. The stability of carbocations is tertiary > secondary > primary [52]. This isomerization reaction is responsible for a high ratio of branched to linear isomers in the products, for example:

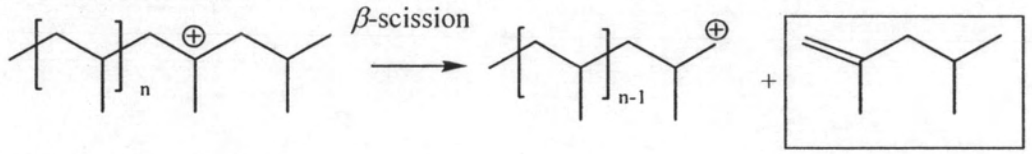

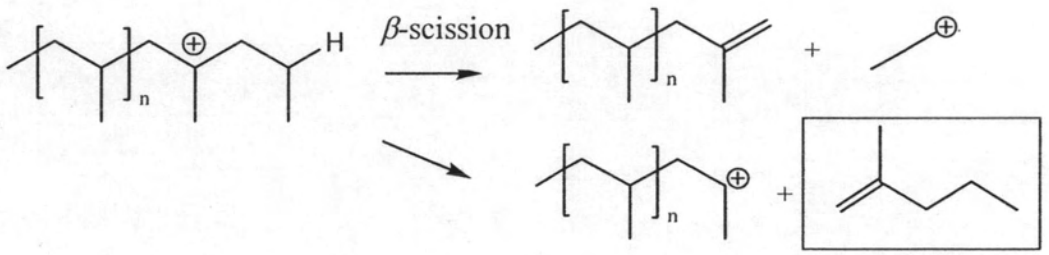

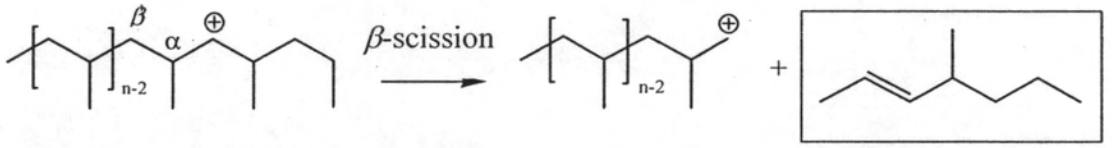

4.6.3 Cyclization of carbocation intermediate

Aromatization of paraffins can occur through a dehydrocyclization reaction. Olefinic compounds formed by β-scission can generate a carbocation intermediate with the configuration readily to undergo cyclization. Possible reaction steps for cyclization are:

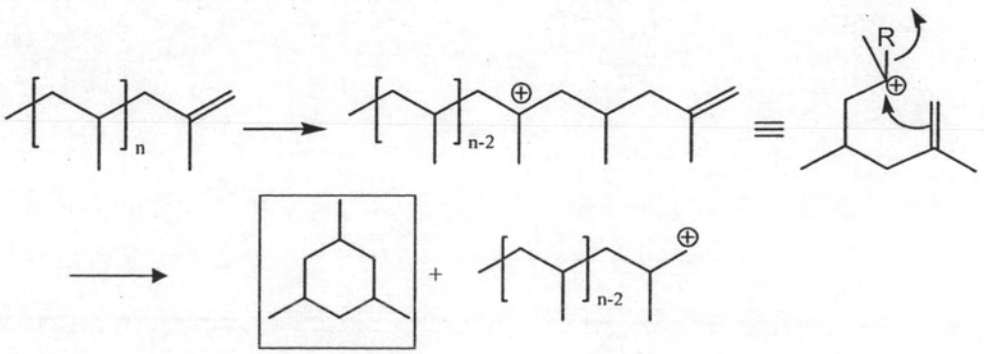

Intramolecular rearrangement via a six-membered transition state to inner tertiary carbon atoms (back biting reaction) can occur to produce 1,3,5-cyclohexane or may be isomerize to form aromatic species.

4.6.4 Addition to olefins

The small fragments in the reaction may be combined together to form larger molecules such as:

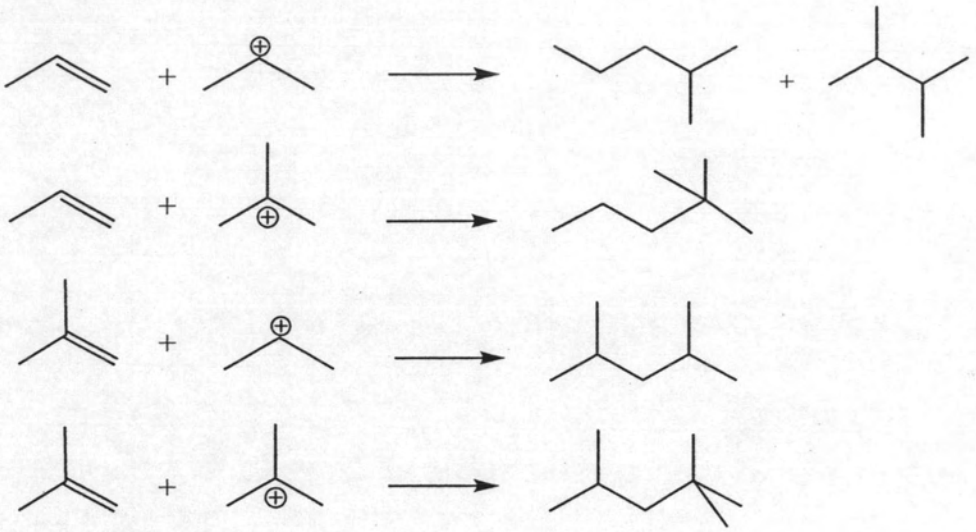

These reactions produce liquid fraction, *i. e.* C6, C7, C8 hydrocarbons. The carbo-cations can be stabilized by various ways such as

- Hydride abstraction from other olefins
- Hydride abstraction from paraffins

The main products of catalytic cracking of polypropylene are propene and isobutene. The catalytic cracking of polypropylene proceeds primarily by means of the following steps: